Syntheses, Crystal Structure and Physico-Chemical Studies of Sodium and Potassium Alcoholates Bearing Thienyl Substituents and their Derived Luminescent Sm(III) Alkoxides

Michael Veith, Céline Belot, Volker Huch, Laurent Guyard, Michael Knorr, Abderrahim Khatyr, Claudia Wickleder

Zeitschrift für Anorganische und Allgemeine Chemie

Syntheses, Crystal Structure and Physico–Chemical Studies of Sodium and Potassium Alcoholates Bearing Thienyl Substituents and their Derived Luminescent Sm(III) Alkoxides

Journal:	*Zeitschrift für Anorganische und Allgemeine Chemie*
Manuscript ID:	zaac.201000205.R1
Wiley - Manuscript type:	Article
Date Submitted by the Author:	27-Jun-2010
Complete List of Authors:	Veith, Michael; INM - Leibniz-Institut für Neue Materialien gGmbh Belot, Céline; Universität des Saarlandes, Institut für Anorganische Chemie Huch, Volker; Universität des Saarlandes, Institut für Anorganische Chemie Guyard, Laurent; Université de Franche–Comté, Institut UTINAM UMR CNRS 6213 Knorr, Michael; Université de Franche–Comté, Institut UTINAM UMR CNRS 6213 Khatyr, Abderrahim; Université de Franche–Comté, Institut UTINAM UMR CNRS 6213 Wickleder, Claudia; University of Siegen, Inorganic Chemistry II
Keywords:	Thienylmethoxido ligands, Hetero-cubanes with alkali metals, Samarium, Electrochemistry, Luminescence

Note: The following files were submitted by the author for peer review, but cannot be converted to PDF. You must view these files (e.g. movies) online.

Figure 1.cdx
Scheme 1.cdx
Scheme 3.cdx

Syntheses, Crystal Structure and Physico–Chemical Studies of Sodium and Potassium Alcoholates Bearing Thienyl Substituents and their Derived Luminescent Sm(III) Alkoxides

Michael Veith,*[a,b] Céline Belot,[a,c] Volker Huch,[a] Laurent Guyard,[c] Michael Knorr,[c] Abderrahim Khatyr[c] and Claudia Wickleder[d]

Abstract. The synthesis, structural characterization, electrochemistry and luminescence properties of a series of alkali metal alcoholates and Sm(III) alkoxides with thiophene–based–OR substituents are presented. The alkali metal alcoholates **7**–**15** have been obtained by deprotonation of the carbinol with NaH or KH. Their molecular structures consist of tetranuclear alkali metal alcoholates with a distorted cubane–like M_4O_4 core (X-ray structure analyses). Each alkali metal is surrounded by three carbinolate ligands and (depending on the derivative) by additional tetrahydrofuran molecules. The mononuclear samarium alkoxides $\{Sm[OC(C_4H_3S)_3]_3(thf)_3\}$ • thf (**16**) and $\{Sm[OC(C_{16}H_{13}S)]_3(thf)_3\}$ • thf (**17**) were synthesized by the salt metathesis reactions between $\{[KOC(C_4H_3S)_3]_4(thf)_2\}$ • thf (**7**), $[NaOC(C_4H_3S)_3]_4(thf)_2$ (**8**) or $\{[KOC(C_{16}H_{13}S)]_4(thf)_3\}$ • ½ thf (**11**), respectively, and $SmCl_3$ in thf solution. The molecular structures of these air–sensitive base adducts have been determined by single–crystal X–ray crystallography and reveal an approximately octahedral coordination sphere around the samarium metal centres with three methoxido ligands and three facially arranged thf molecules. The electrochemical properties are essentially dominated by the oxidation of the thienyl units. The emission spectra of the carbinols and their derived potassium and sodium compounds display broad bands attributed to the $\pi^* \rightarrow \pi$ transitions of the aromatic ligands. Luminescence studies performed on complexes **16** and **17**

* Prof. Dr. Dr. h. c. M. Veith
E-Mail: Michael.Veith@inm-gmbh.de
[a] Institut für Anorganische Chemie
Universität des Saarlandes
Postfach 15 11 50
66041 Saarbrücken, Germany
[b] INM - Leibniz Institute for New Materials
Campus D2 2
66123 Saarbrücken, Germany
[c] Institut UTINAM UMR CNRS 6213
Université de Franche–Comté
16, Route de Gray,
25030 Besançon, France
[d] Inorganic Chemistry II
University of Siegen
Adolf–Reichwein–Straße
57068, Siegen, Germany

reveal the typical f–f transitions of the Sm(III) ion. The photophysical data suggest that an energy transfer from the ligand to the metal centre operates.

Keywords: Thienylmethoxido ligands; Hetero-cubanes with alkali metals; Samarium; Electrochemistry; Luminescence

Introduction

Trivalent lanthanide compounds have received much attention within the last decade because of their luminescence properties and their applications in electronic materials and in biological systems [1]. The intraconfigurational 4f–4f transitions are parity forbidden and their emission and absorption spectra exhibit weak intensity upon an excitation on the lanthanide ion. However, some organic ligands can act as an "antenna", absorbing and transferring energy efficiently to the metal ion and consequently increasing their luminescence yield [2]. The choice of the ligand for complexation plays a key role in constructing efficient luminescence lanthanides complexes. Two common requirements for selecting a ligand for the coordination with lanthanide ions are the metal binding strength and ultraviolet (UV) absorption properties of ligands. Among several categories of ligands, nitrogen– and oxygen–donor groups have been used in the sensitization of lanthanide luminescence. In particular, bidendate aromatic amines, carboxylic acids and *β*–diketonates are known to provide energy transfer to lanthanides ions [3]. However, to date only a few examples of lanthanide complexes bearing sulphur moieties has been reported [4–6] probably due to the generally lower stability and the mismatch between a soft sulfur–donor ligand and a hard lanthanide metal ion. In particular, those containing thienyl rings have been barely explored, although their transition metal counterparts have been investigated in detail [7]. This interest stems from the fact that thiophene derivatives are quite attractive as organic ligands because of their electron–rich system and their electroactive character.

Complexes containing Sm(III) have been less studied than those with Eu(III) and Tb(III), since they generally exhibit lower intensity for the luminescence. But, trivalent samarium ions present an orange–red emission in the spectral region [8, 9], and have been investigated in light–converting devices together with Eu(III) and Tb(III) analogues [9b, 9h]. Moreover, trivalent samarium(III) derivatives may have attractive catalytic activity: they can act as Lewis acid to activate Michael–aldol reaction [10], epoxidation of alcohols [11], Meerwein–

Ponndorf–Verley–Oppenauer reaction, aldol reaction [11], Diels–Alder reaction [12] and Tischenko reaction [13]. For example, Imamoto *et al.* [14] have recently used the trivalent alkoxide complex Sm(III)tris(2,6–di–*tert*–butyl–4–methylphenoxides) to catalyze Michael–Michael–aldol–reaction of 3,3–dimethyl–2–butanone with benzalacetophenone.

In two previous papers, we have studied the synthesis and physico–chemical properties of a series of rare earth alkoxides of Y and Nd bearing thiophene moieties [5, 6]. We present herein the syntheses of two novel samarium(III) alkoxides, their structural characterisation as well as electrochemical and photoluminescence properties. A strategy that we have developed recently consists of the preparation of suitable tertiary alcohols with thienyl and phenyl substituents capable of being attached on rare earth metal centres through a covalent M–O–R bond, leading to coordination compounds with singular redox and luminescence properties. Furthermore, we have investigated the deprotonation of the bulky and slightly acidic tertiary alcohol shown in Figure 1 using potassium and sodium hydride as bases. The resulting salts have been characterized crystallographically. Furthermore, they have been used for the synthesis of derivatives of samarium (III). In addition, the electrochemical and luminescence properties of all these new compounds have been explored.

Experimental Section

Materials. All reactions were performed under nitrogen atmosphere in a Schlenk apparatus. Tetrahydrofuran and diethyl ether were distilled from sodium and kept under nitrogen. Dichloromethane and acetonitrile were distilled from $CaCl_2$ and kept under nitrogen. Tris(2–thienyl)methanol (**1**), phenylbis(2–thienyl)methanol (**2**), diphenyl(2–thienyl)methanol (**3**), phenylbis(3–thienyl)methanol (**5**) and diphenyl(3–thienyl)methanol (**6**) were prepared according to the literature [15].

HO–C($C_{17}H_{15}S$) (4): To a solution of 2–methylthiophene (1.57 g, 16 mmol, 1.53 mL) in diethyl ether (20 mL) was added *n*–butyl lithium (16 mmol, 10 mL, 1.6 M solution in hexane) at –15°C. The solution was stirred for 1 h, and then benzophenone (2.91 g, 16 mmol) in diethyl ether was added, and the mixture was allowed to reach room temperature and was stirred overnight. It was hydrolysed with an aqueous saturated sodium hydrogenocarbonate

solution. The mixture was extracted with diethyl ether, and the organic layer was dried over Na_2SO_4 and evaporated. The solid was washed in hexane. A white solid was obtained (yield 67 %, 3 g). ^{1}H–NMR ($CDCl_3$): δ 7.3 (m, 10H, Ph), 6.5 (m, $^3J_{H4–H3}$ = 3.4 Hz and $^4J_{H4–HMe}$ = 1.03 Hz, 1H, 4–H Th), 6.4 (d, $^3J_{H3–H4}$ = 3.4 Hz, 1H, 3–H Th), 2.9 (br s, 1H, –O*H*), 2.4 (d, $^4J_{HMe–H4}$ = 0.7 Hz, 3H, –CH_3). ATR–IR: $\bar{\nu}$ (OH) = 3448 cm^{-1}. Anal. Calcd for $C_{18}H_{16}OS$ C, 77.14; H 5.71; Found C, 77.10; H, 4.46.

General Procedure for Preparation of Potassium Alcoholates 7, 9, 11 and 12

The carbinols (1.39 g of **1**; 1.37 g of **2**, 1.471 g of **3**; 1.431 g of **4** (5.0 mmol)) were dissolved in thf (20 mL) and slowly added to a suspension of KH (0.202 g, 5.0 mmol) in thf (5 mL). The mixture was stirred at room temperature overnight. All the KH had reacted. The solvents were evaporated, and solids were obtained from which colourless crystals can be formed in thf at 5°C.

{[KOC(C$_4$H$_3$S)$_3$]$_4$(thf)$_2$} • thf (7): Yield 20 % (362 mg). ^{1}H–NMR (thf/C_6D_6): δ 6.9 (dd, $^3J_{H5–H4}$ = 4.7 Hz and $^4J_{H5–H3}$ = 1.3 Hz, 12H, 5–H), 6.8 (dd, $^3J_{H3–H4}$ = 3.3 Hz and $^4J_{H3–H5}$ = 1.3 Hz, 12H, 3–H), 6.7 (dd, $^3J_{H4–H3}$ = 3.3 Hz and $^3J_{H4–H5}$ = 4.7 Hz, 12H, 4–H). Anal. Calcd for $C_{64}H_{60}O_7S_{12}K$ C, 51.81; H, 4.05; Found C, 53.02; H 3.31.

[KOC(C$_{14}$H$_{11}$S$_2$)]$_4$(thf)$_3$ (9): Yield 30 % (580 mg). ^{1}H–NMR (thf/C_6D_6): δ 7.5 (m, 8H, 5–H Th), 6.9 (m, 20H, Ph), 6.7 (m, 8H, 4–H Th), 6.5 (m, 8H, 3–H Th). Anal. Calcd for $C_{72}H_{68}O_7S_8K_4$ C, 59.25; H, 4.66; cannot be performed because of the sensibility.

{[KOC(C$_{16}$H$_{13}$S)]$_4$(thf)$_3$} • ½ thf (11): Yield 34 % (610 mg). ^{1}H–NMR (thf/C_6D_6): δ 7.3 (m, 12H, 5–H Th, Ph), 6.9 (m, 32H, Ph), 6.7 (m, 4H, 4–H Th), 6.4 (m, 4H, 3–H Th). Anal. Calcd for $C_{82}H_{80}O_{7.5}S_4K_4$ C, 67.02; H, 5.40; Found C, 65.74; H, 4.60.

[KOC(C$_{17}$H$_{15}$S)]$_4$(thf)$_2$ (12): Yield 29 % (515 mg). ^{1}H–NMR (thf/C_6D_6): δ 7.3 (m, 16H, Ph), 7.0 (m, 24H, Ph), 6.4 (m, 4H, 4–H Th), 6.2 (m, 4H, 3–H Th), 2.2 (s, 12H, –CH_3). Anal. Calcd for $C_{80}H_{76}O_6S_4K_4$ C, 67.69; H, 5.35; Found C, 66.60; H, 6.60.

General Procedure for Preparation of Sodium Alcoholates 8, 10, 13–15

The carbinols (1.40 g of **1**; 1.37 of **2**; 1.42 g of **4**; 1.367 g of **5**; 1.338 g of **6** (5.0 mmol)) were dissolved in thf (20 mL) and slowly added to a suspension of NaH (0.121g, 5 mmol) in thf (5 mL). The mixture was stirred at room temperature overnight.

[NaOC(C$_4$H$_3$S)$_3$]$_4$(thf)$_2$ (8): All NaH had reacted. The solvent was evaporated; a solid was obtained from which colourless crystals could be obtained in thf at 5°C (yield: 15 %, 243 mg). ^{1}H–NMR (thf/C_6D_6): δ 6.9 (dd, $^3J_{H5–H4}$ = 4.9 Hz and $^4J_{H5–H3}$ = 1.2 Hz, 12H, 5–H), 6.8

(dd, $^{3}J_{H3–H4}$ = 3.4 Hz and $^{4}J_{H3–H5}$ = 1.2 Hz, 12H, 3–H), 6.7 (dd, $^{3}J_{H4–H3}$ = 3.7 Hz and $^{3}J_{H4–H5}$ = 4.9 Hz, 12H, 4–H). Anal. Calcd for $C_{60}H_{52}O_6S_{12}Na_4$ C, 53.50; H, 3.86; Found C, 52.24; H, 3.56.

$[NaOC(C_{14}H_{11}S_2)]_4(thf)_2$ (10): The unreacted NaH was filtered. The solvent was slowly evaporated, a light–brown solid precipitated, which was separated from the liquid residue. The isolated yield is 32 % (529 mg). ^{1}H–NMR (thf/C_6D_6): δ 7.6 (dd, $^{3}J_{H5–H4}$ = 6.6 Hz and $^{4}J_{H5–H3}$ = 1.3 Hz, 8H, 5–H Th), 7.0 (m, 28H, 4–H, Ph), 6.7 (dd, $^{3}J_{H4–H3}$ = 4.0 Hz , 8H, 3–H Th). Anal. Calcd for $C_{68}H_{60}O_6S_8Na_4$: C, 61.81; H, 4.54; Found C, 60.61; H, 4.39.

$[NaOC(C_{17}H_{15}S)]_4(thf)_2$ (13): The suspension turned into a solution. The solvent was slowly evaporated, a white solid precipitated, which was filtered (yield 14 %, 241 mg). ^{1}H–NMR (thf/C_6D_6): δ 7.3 (m, 16H, Ph), 7.0 (m, 24H, Ph), 6.4 (m, 4H, 4–H Th), 6.2 (m, 4H, 3–H Th), 2.2 (s, 12H, –CH_3). Anal. Calcd for $C_{80}H_{76}O_6S_4Na_4$ C, 71.00; H, 5.62; Found C, 71.00; H, 5.59.

$[NaOC(C_{14}H_{11}S_2)]_4(thf)_2$ (14): The unreacted NaH was filtered. The solvent was slowly evaporated; colourless crystals were obtained (yield 22 %, 362 mg). ^{1}H–NMR (thf/C_6D_6): δ 7.2 (m, 16H, Ph, 5–H Th), 7.0 (m, 12H, Ph), 6.8 (m, 8H, 4–H Th), 6.2 (m, 8H, 2–H Th). Anal. Calcd for $C_{68}H_{60}O_6S_8Na_4$ C, 61.81; H, 4.54; Found C, 59.54; H, 5.08.

$[NaOC(C_{16}H_{13}S)]_4(thf)_2$ (15): The reaction mixture was filtered, and the solvent was slowly evaporated, from which a white solid precipitated (yield 31 %, 490 mg). ^{1}H–NMR (thf/C_6D_6): δ 7.3 (m, 12H, Ph, 5–H Th), 7.0 (m, 24H, Ph), 6.9 (d, 4H, 4–H Th), 6.2 (s, 4H, 2–H Th). Anal. Calcd for $C_{76}H_{68}O_6S_4Na_4$ C, 70.37; H, 5.24; Found C 71.03; H, 5.09.

$\{Sm[OC(C_4H_3S)_3]_3(thf)_3\} \cdot thf$ (16):

Method 1: To a suspension of NaH (0.104 g, 4.3 mmol) in thf (5 mL) was slowly added tris(2–thienyl)methanol (1.21 g, 4.3 mmol) in thf (20 mL). The mixture was stirred at room temperature overnight. Then, it was added to a suspension of $SmCl_3$ (0.373 g, 1.4 mmol) in thf (5 mL). The mixture was stirred at room temperature for two days. NaCl was filtered. The solution was concentrated and brown–light crystals were obtained at 5°C a few days later. The isolated yield is 24 % (430 mg).

Method 2: To a suspension of KH (0.154 g, 3.8 mmol) in thf (5 mL) was slowly added Tris(2–thienyl)methanol (1.07 g, 3.8 mmol) in thf (20 mL). The mixture was stirred at room temperature overnight. Then, it was added to a suspension of $SmCl_3$ (0.328 g, 1.3 mmol) in thf (5 mL). The mixture was stirred at room temperature for two days. KCl was filtered. The

solution was concentrated and brown–light crystals were obtained at 5°C after a few days. The isolated yield is 13 % (217 mg).
^{1}H–NMR ($CDCl_3$): δ 7.2 (br. s, 27H, 3–H, 4–H, 5–H), 3.6 (br. s, 8H, thf), 3.4 (br. s, 3H, thf), 1.7 (br s, 10H, thf), 1.2 (br. s, 8H, thf), 0.9 (br s, 3H, thf). Anal. Calcd for $C_{55}H_{59}O_7S_9Sm$ C, 51.93; H, 4.64; Found C, 49.32; H, 4.57.

$\{Sm[OC(C_{16}H_{13}S)]_3(thf)_3\} \cdot thf$ (17): To a suspension of KH (0.193 g, 4.8 mmol) in thf (5 mL) was slowly added diphenyl(2–thienyl)methanol (1.28 g, 4.8 mmol) in thf (20 mL). The mixture was stirred at room temperature overnight. Then, it was added to a suspension of $SmCl_3$ (0.410 g, 1.6 mmol) in thf (5 mL). The mixture was stirred at room temperature for two days. KCl was filtered. The solution was concentrated and colourless crystals were obtained at 5°C few days later. The isolated yield is 10 % (190 mg). ^{1}H–NMR ($CDCl_3$): δ 7.3 (m, 33 H, Ph, 5–H Th), 6.9 (dd, 3 H, 4–H Th, $^3J_{H4–H5}$ = 5.14 Hz , $^3J_{H4–H3}$ = 3.97 Hz,), 6.7 (dd, 3 H, 3–H Th, $^3J_{H3–H4}$ = 3.42 Hz , $^3J_{H3–H5}$ = 1.22 Hz, ,), 3.7 (m, 12 H, thf), 1.8 (m, 12 H, thf) ppm. Anal. Calcd for $C_{67}H_{71}O_7S_3Sm$ C, 65.11; H 5.75; Found C, 65.18; H, 6.19.

Instruments. The ^{1}H NMR spectra were recorded on a Bruker ACF–NMR (200 MHz) for **4** and **7**–**15** and Bruker Avance 400 spectrometer (400 MHz, H,H–COSY) for **16**–**17**. All chemical shifts (δ) and coupling constants (J) are given in ppm and Hertz, respectively. Analytical data were measured with a LECO CHN–900 instrument. The ATR–IR spectra were performed using a Bruker Vector 22 Spectrometer equipped with Golden Gate.

Electrochemistry. Cyclic voltammetric experiments were performed on an Autolab PGSTAT 20 Potentiostat Galvanostat (Ecochemie) equipped with a three–electrode assembly with 0.1 M $[NBu_4][PF_6]$ (TBAF) as supporting electrolyte and CH_3CN or CH_2Cl_2 as solvent. The working electrode was a platinum disk of 1 mm in diameter; it was polished consecutively with polishing alumina and diamond suspension between the runs. The reference electrode was $Ag/AgClO_4$ (0.1 M in CH_3CN). A platinum disk was used as an auxiliary electrode. The solvent was freshly distilled, and the solutions were prepared under nitrogen atmosphere and blanketed with N_2 before the first scan. Measurements were made at room temperature. The scan rates employed were 100 $mV.s^{-1}$. The concentration of the monomeric substrates was 10^{-3} M for the carbinol and alkali metal alcoholates and approximately 3.15×10^{-3} M for **16** and 3.32×10^{-3} M for **17**. Under these conditions, the $E_{1/2}$ of $Cp_2Fe^{+/0}$ was found to be 0.16 V (CH_2Cl_2) and 0.025 V (CH_3CN) vs. an $Ag/AgClO_4$ reference.

Luminescence studies. Solid–state emission and excitation spectra were recorded at room temperature on a Jobin–Yvon Fluorolog–3 spectrometer equipped with a 1000 w Xenon lamp, two double grated monochromators for emission and excitation, respectively, and a photomultiplier with a photon counting system. The emission spectra were corrected for photomultiplier sensitivity, the excitation spectra for lamp intensity and both for the transmission of the monochromators.

Crystallography. The data collection was performed on a X8 ApexII CCD diffractometer with MoKα radiation (λ = 0.71073 Å). Structures were solved by direct methods and refined by full–matrix least square methods on F^2 with SHELX–97 [16]. Drawings were made with Diamond [17]**.** All crystals of the compounds started growing up at 5°C during a period of one week. No sign of deterioration during storage under nitrogen was observed. Crystallographic data for the structure determinations are listed in Table 1, and relevant bond distances and angles are given in Tables 3–6. Most of the alkali compounds (**7**, **8**, **9**, **12**) had weak reflections at higher theta values which explains the bad R-values. The structures **9** and **12** are only generally discussed without looking into the details of bonding. Under CCDC 776395 - 776401 supplementary crystallographic data for the compounds are deposited. These data can be obtained free of charge from The Cambridge Crystallographic Data Centre via www.ccdc.cam.ac.uk/data_request/cif.

Table 1. X–ray crystallographic and refinement data for **7**–**9**, **11**–**12** and **16**–**17**.

Compounds	**7**	**8**	**9**	**11**	**12**	**16**	**17**
Empirical formula	$C_{64}H_{60}K_4O_7S_{12}$	$C_{60}H_{52}Na_4O_6S_{12}$	$C_{72}H_{68}K_4O_7S_8$	$C_{84}H_{82}K_4O_{7.5}S_3$	$C_{80}H_{76}K_4O_6S_4$	$C_{55}H_{59}O_7S_9Sm$	$C_{67}H_{71}O_7S_3Sm$
Formula weight	1482.24	1345.70	1458.14	1464.08	1418.05	1270.91	1234.77
Temperature [K]	103(2)	103(2)	130(2)	130(2)	130(2)	130(2)	130(2)
Crystal system	Orthorhombic	Monoclinic	Monoclinic	Cubic	Monoclinic	Rhombohedral	Trigonal
Space group	Pccn	C2/c	C2/c	P2(1)3	C2/c	R3	P31c
a [Å]	14.246(1)	23.19(1)	24.77(1)	24.494(1)	23.647(1)	13.940(1)	14.568(1)
b [Å]	16.743(1)	13.343(1)	24.21(1)	24.4944(1)	14.219(1)	13.940(1)	14.568(1)
c [Å]	27.71(1)	22.98(1)	49.109(3)	24.494(1)	42.900(2)	24.700(4)	15.780(1)
α [°]	90	90	90	90	90	90	90
β [°]	90	119.96(1)	91.55(1)	90	94.10(1)	90	90
γ [°]	90	90	90	90	90	120	120
Volume [$Å^3$]	6608.6(6)	6158.8(5)	29444(3)	14695.9(6)	14387(1)	4156.8(8)	2900.4(3)
Z	4	4	16	8	8	3	2
ρ_{calc} [mg/m^3]	1.490	1.451	1.316	1.323	1.309	1.523	1.414
μ [mm^{-1}]	0.701	0.504	0.519	0.384	0.416	1.450	1.175
F(000)	3072	2784	12160	6160	5952	1953	1278
Crystal size [mm^3]	0.55x0.3x0.25	0.4x0.28x0.22	0.55x0.37x0.22	0.5x0.2x0.09	0.42x0.40x0.29	0.3x0.44x0.5	0.50x0.37x0.06
Theta range for data collection [°]	1.47 to 29.40	1.83 to 34.67.	1.18 to 26.49	1.18 to 28.26	1.67 to 26.44	1.88 to 34.27	1.61 to 26.41
Reflexion collected	46554	105170	123598	83983	117135	26806	16454

Independent reflections	9114 [R(int) = 0.0290]	12917 [R(int) = 0.0356]	30203 [R(int) = 0.0765]	12157 [R(int) = 0.1092]	14786 [R(int) = 0.0406]	5629 [R(int) = 0.0350]	3955 [R(int) = 0.0397]
Completeness to theta [%]	99.9 (29.40°)	97.5 (34.67°)	99.1 (26.49°)	100.0 (28.26°)	99.7 (26.44°)	99.9 (34.27)°	100.0 (26.21°)
Absorption correction	None	Multiscan	Multiscan	None	Multiscan	Multiscan	Multiscan
Data / restraints / parameters	9114 / 0 / 460	12917 / 0 / 360	30203 / 4 / 1671	12157 / 0 / 589	14786 / 13 / 874	5629 / 1 / 216	3955 / 1 / 209
Goodness–of–fit on F^2	2.785	2.755	2.076	1.022	1.228	1.433	1.375
Final R indices [I>2sigma(I)]	R1 = 0.0951, wR2 = 0.2853	R1 = 0.1052, wR2 = 0.2969	R1 = 0.1224, wR2 = 0.3011	R1 = 0.0626, wR2 = 0.1497	R1 = 0.1107, wR2 = 0.2368	R1 = 0.0482, wR2 = 0.1311	R1 = 0.0490, wR2 = 0.1275
Largest diff. Peak and hole [e·Å^{-3}]	2.130 and –1.303	4.195 and –2.547	1.207 and –1.201	1.010 and –0.516	1.386 and −1.718	2.826 and −1.752	0.916 and −0.416

Results and Discussion

Samarium(III) alkoxides have been prepared in the past by transesterification reactions of Sm–O*i*Pr in the presence of an excess of other alcohols R'OH to provide Sm–OR' species [18]. Mononuclear phenoxide and siloxides of type $Sm(OAr)_3(thf)_3$ and $Sm(OSiPh)_3(thf)_3$ were also obtained by alcoholysis of the dinuclear organometallic samariumfluoride $[\{-(Me_3Si)_2C_5H_3\}_2SmF]_2$ in the presence of slightly acidic ArOH or Ph_3SiOH [19]. Reaction of equimolar quantities of $Sm[N(SiMe_3)_2]_3$ and $Al(i\text{–}Bu)_3$ in the presence of *i*–propanol or *t*–BuOH allowed the preparation of the mixed–metal alkoxide complexes $\{[(i\text{–}Pr\text{–}O)(i\text{–}Bu)Al(\mu\text{–}O\text{–}i\text{–}Pr)_2Sm(O\text{–}i\text{–}Pr)(HO\text{–}i\text{–}Pr)](\mu\text{–}O\text{–}i\text{–}Pr)\}_2$. An analogous reaction between $Sm[N(SiMe_3)_2]_3$, $Al(i\text{–}Bu)_3$ and *t*–BuOH, followed by addition of thf, produced the thf adduct $[(thf)_2Sm(O\text{–}t\text{–}Bu)_2(\mu\text{–}O\text{–}t\text{–}Bu)_2Al(i\text{–}Bu)_2]$ [20]. But the most classical route to prepare samarium alkoxides and those of other lanthanides is the salt elimination by reaction between alkali metal alcoholates and a lanthanide halide [21].

*Synthesis of the carbinol **4***

The hitherto unknown compound diphenyl(5–methyl–2–thienyl)methanol (**4**) was prepared by a similar method as employed for the synthesis of other carbinols [15]. This colourless solid was obtained by a classical nucleophilic addition of lithiated 2–methylthiophene on benzophenone according Scheme 1 and isolated in 67 % yield after subsequent hydrolysis and workup. The ^{1}H–NMR spectrum of **4**, recorded in chloroform, displays three aromatic signals: a multiplet at 7.3 ppm attributed to the protons of the phenyl groups, a multiplet at δ 6.5 and a doublet at 6.4 ppm of the 4–H and the 3–H of the thienyl unit, respectively. A broad signal at 2.9 ppm due to the alcohol function is also obtained. The latter signal, a doublet at δ 2.4, is assigned to the protons of the methyl group.

Synthesis and Characterisation of the Potassium and Sodium Thienyl–Substituted Alcoholates

We have recently prepared a series of mononuclear lanthanide carbinol complexes bearing thienyl substituents of type $Ln(OR)_3(thf)_n$ (Ln = Nd, Er) by the above mentioned aminolysis reaction of silylamides $Ln[N(SiMe_3)_2]_3$ in the presence of thienyl–functionalized carbinols [5, 6]. Unfortunately, we failed to isolate any Sm(III) complexes in crystalline form using this

route. For this reason we have chosen the salt–elimination route to prepare the targeted samarium complexes.

The targeted potassium or sodium alcoholates **7**–**15** have been synthesized straightforwardly by deprotonation of the corresponding carbinol with potassium or sodium hydride according Scheme 2. In the course of all reactions, which were conducted at room temperature overnight, hydrogen gas developed. The compounds $\{[KOC(C_4H_3S)_3]_4(thf)_2\}$ • thf (**7**), $[NaOC(C_4H_3S)_3]_4(thf)_2$ (**8**) $[KOC(C_{14}H_{11}S_2)]_4(thf)_3$ (**9**), $\{[KOC(C_{16}H_{13}S)]_4(thf)_3\}$ • ½ thf (**11**) and $[KOC(C_{17}H_{15}S)]_4(thf)_2$ (**12**) can be isolated as colourless crystals, whose crystallographic characterisation (see below) revealed their tetranuclear nature. The ^{1}H–NMR spectra of these alcoholates recorded in thf/C_6D_6, show the typical aromatic signals of thienyl and/or phenyl groups (Table 2). Unfortunately, we failed to grow single crystals of **10** and **13**–**15.** According to the ^{1}H–NMR spectra (Table 2), we presume that NaH and the carbinols **2** and **5**–**6** react in the same manner as the other derivatives and postulate tentatively a tetrameric cage structure for the isolated solids with composition $[NaOC(C_{14}H_{11}S_2)]_4(thf)_2$ (**10**), $[NaOC(C_{17}H_{15}S)]_4(thf)_2$ (**13**), $[NaOC(C_{14}H_{11}S_2)]_4(thf)_2$ (**14**) and $[NaOC(C_{16}H_{13}S)]_4(thf)_2$ (**15**). The number of thf molecules coordinated to the clusters follows from chemical analysis (see exp. section).

Table 2. ^{1}H–NMR chemical shifts for the alkali metal alcoholates **7**–**15** obtained in thf/C_6D_6.

Compounds	Chemical Shifts
7	6.9 (dd, $^3J_{H5–H4}$ = 4.7 Hz and $^4J_{H5–H3}$ = 1.3 Hz, 12H, 5–H), 6.8 (dd, $^3J_{H3–H4}$ = 3.3 Hz and $^4J_{H3–H5}$ = 1.3 Hz, 12H, 3–H), 6.7 (dd, $^3J_{H4–H3}$ = 3.3 Hz and $^3J_{H4–H5}$ = 4.7 Hz, 12H, 4–H)
8	6.9 (dd, $^3J_{H5–H4}$ = 4.9 Hz and $^4J_{H5–H3}$ = 1.2 Hz, 12H, 5–H), 6.8 (dd, $^3J_{H3–H4}$ = 3.4 Hz and $^4J_{H3–H5}$ = 1.2 Hz, 12H, 3–H), 6.7 (dd, $^3J_{H4–H3}$ = 3.7 Hz and $^3J_{H4–H5}$ = 4.9 Hz, 12H, 4–H)
9	7.5 (m, 8H, 5–H Th), 6.9 (m, 20H, Ph), 6.7 (m, 8H, 4–H Th), 6.5 (m, 8H, 3–H Th)
10	7.6 (dd, $^3J_{H5–H4}$ = 6.6 Hz and $^4J_{H5–H3}$ = 1.3 Hz, 8H, 5–H Th), 7.0 (m, 28H, 4–H, Ph), 6.7 (dd, $^3J_{H4–H3}$ = 4.0 Hz , 8H, 3–H Th)
11	7.3 (m, 12H, 5–H Th, Ph), 6.9 (m, 32H, Ph), 6.7 (m, 4H, 4–H Th), 6.4 (m, 4H, 3–H Th)
12	7.3 (m, 16H, Ph), 7.0 (m, 24H, Ph), 6.4 (m, 4H, 4–H Th), 6.2 (m, 4H, 3–H Th), 2.2 (s, 12H, –CH_3)
13	7.3 (m, 16H, Ph), 7.0 (m, 24H, Ph), 6.4 (m, 4H, 4–H Th), 6.2 (m, 4H, 3–H Th), 2.2 (s, 12H, –CH_3)
14	7.2 (m, 16H, Ph, 5–H Th), 7.0 (m, 12H, Ph), 6.8 (m, 8H, 4–H Th), 6.2 (m, 8H, 2–H Th)
15	7.3 (m, 12H, Ph, 5–H Th), 7.0 (m, 24H, Ph), 6.9 (d, 4H, 4–H Th), 6.2 (s, 4H, 2–H Th)

Crystallographic Characterisation of the Thienyl–Substituted Alcoholates

An important number of X–ray structure determinations on the alkali metal alcoholates have revealed a rich diversity of solid–state structures for these salts. Known examples show as motif dimers, trimers, cubane–like tetramers, face fused cubic tetramers and hexamers [22-25].

We succeeded in growing colourless single crystals suitable for X–ray structure determinations for compounds **7**–**9** and **11**–**12** from thf solution at 5°C. All structure determinations reveal the presence of tetrameric alkali metal alcoholates with a distorted cubane–like M_4O_4 core (M = K or Na), whose most salient metric parameters are presented below. Some of the structures, besides their bad diffraction behaviour, suffer from disordering of the thienyl ligands.

For the potassium alcoholates **7** and **11**, selected bond lengths and angles are gathered in Tables 3–4. The asymmetric unit of **11** contains two crystallographically independent molecules (**A** and **B**) having very close geometries (see Table 4). Herein, we will only refer to the molecule **A**. Unfortunately, for the compounds **9** and **12**, no discussion or comparison of the bond lengths and angle values is meaningful due to the poor quality of the crystals (high R–values).

Table 3. Selected bond lengths /Å and angles /° for Compound **7**.

7			
K(1)–O(2)	2.671(3)	K(2)–O(3)	2.687(4)
K(1)–O(1)	2.636(3)	K(2)••••K(1)	3.611(1)
K(2)–O(1)	2.652(4)	K(2)••••K(2)	3.855(2)
K(2)–O(2)	2.736(3)		
K(1)–O(2)–K(1)	87.67(9)	O(1)–K(2)–O(2)	89.7(1)
K(1)–O(2)–K(2)	87.90(9)	O(1)–K(2)–O(1)	87.1(1)
K(1)–O(1)–K(2)	90.4(1)	O(3)–K(2)–O(2)	127.4(1)
K(2)–O(1)–K(2)	92.6(1)	C(1)–O(1)–K(1)	119.1(3)
O(2)–K(1)–O(2)	91.6(1)	C(1)–O(1)–K(2)	126.6(3)
O(1)–K(1)–O(2)	91.5(1)	C(14)–O(2)–K(2)	141.3(2)
O(1)–K(2)–O(3)	118.5(1)	C(14)–O(2)–K(1)	128.5(2)

Table 4. Selected bond lengths /Å and angles /° for {[KOC($C_{16}H_{13}S$)]$_4$(thf)$_3$} • ½ thf (**11**) (molecules **A** and **B**).

A		**B**	
K(1)–O(1)	2.789(3)	K(3)–O(3)	2.790(3)
K(2)–O(1)	2.625(3)	K(4)–O(3)	2.702(3)
K(2)–O(2)	2.696(3)	K(4)–O(4)	2.667(3)
K(2)–O(5)	2.765(4)	K(4)–O(6)	2.742(4)
O(2)–C(18)	1.390(9)	O(4)–C(46)	1.400(8)
K(2)••••K(2)	3.754(2)	K(4)••••K(4)	3.734(2)
K(2)–O(1)–K(1)	88.50(9)	K(4)–O(3)–K(3)	86.67(9)
K(2)–O(1)–K(2)	88.3(1)	K(4)–O(4)–K(4)	88.9(1)
O(1)–K(1)–O(1)	91.95(9)	O(3)–K(3)–O(3)	91.35(9)
O(1)–K(2)–O(1)	94.8(1)	O(3)–K(4)–O(6)	126.7(1)
O(1)–K(2)–O(2)	94.37(9)	O(3)–K(4)–O(4)	124.3(1)
O(1)–K(2)–O(5)	115.9(1)	O(3)–K(4)–O(6)	124.3(1)
O(2)–K(2)–O(5)	113.9(1)	O(4)–K(4)–O(6)	117.9(1)
O(5)–K(2)–O(1)	137.9(1)	C(29)–O(3)–K(3)	115.6(2)
C(1)–O(1)–K(1)	113.4(2)	C(29)–O(3)–K(4)	119.0(2)
C(1)–O(1)–K(2)	146.0(2)	C(46)–O(4)–K(4)	126.07(8)
C(18)–O(2)–K(2)	126.45(8)		

The molecular structures of **7**, **9**, **11** and **12** exhibit tetrameric units: each potassium atom is surrounded by three carbinolato ligands. In addition, two or three alkali metals are also coordinated to a tetrahydrofuran molecule (Figure 2a), 3a) and 4).

The molecular units {[KOC(C_4H_3S)$_3$]$_4$(thf)$_2$} (**7**) and {[KOC($C_{16}H_{13}S$)]$_4$(thf)$_3$} (**11**) are situated on a C_2 and C_3 axis in the crystal, respectively. Tetrahydrofuran molecules are present in the crystal lattices without interaction with the central motif. The geometry in **7** and **11** around K(1), in a first approximation, is trigonal pyramidal and these for K(2) tetrahedral. These molecular structures resemble those found for [K(μ_3–DPE)(thf)]$_4$ or [K(μ_3–DPE)(py)]$_4$ • 2 py [25]. The potassium-oxygen mean distances are found to be 2.673(4) Å (**7**) and 2.703(3) Å (**11**) and are in the range reported for [K(μ_3–DPE)(thf)]$_4$ [2.641(0) and 2.720(2) Å] and [K(μ_3–DPE)(py)]$_4$ • 2 py [2.653(8) Å] [25]. The K–O bond lengths between K(2) and the oxygen atom of the tetrahydrofuran molecule of 2.687(4) Å (**7**) and 2.765(4) Å (**11**) are in agreement with those observed for [K(μ_3–DPE)(thf)]$_4$ [2.720(2) Å] [25]. The presence of the

solvent molecules coordinated only with two (**7**) or three (**11**) potassium atoms leads to a deformation of the heterocubane core, as can be deduced from the O-K-O angles.

Apparently, not all the potassium atoms are ligated to a solvent molecule: two atoms for **7** and **12** and one atom for **9** and **11** have no base coordination. A closer view to the surrounding of these atoms shows that the thienyl or phenyl rings are shielding the metal in a π–ligand manner preventing the possible addition of a third (**7** and **12**) or a fourth (**9** and **11**) tetrahydrofuran molecule (Figure 2b) and 3b) and 4). Note that the K–S distances are between 3.251(9) and 5.518(6) Å and therefore a coordination of sulphur to potassium is very weak, if any.

We also elucidated the crystal structure of the sodium salt $[NaOC(C_4H_3S)_3]_4(thf)_2$ (**8**). Like in the case of the potassium analogue (see above), the molecular structure of $[NaOC(C_4H_3S)_3]_4(thf)_2$ (**8**) consists of a tetrameric motif with a distorted cubane–like arrangement (Figure 5). This molecular cluster is situated on a C_2 axis in the crystal. In contrast to $\{[KOC(C_4H_3S)_3]_4(thf)_2\}$ • thf (**7**), the Na(1) atoms are surrounded by the three tris(2–thienyl)methanolato ligands and additionally ligated by a sulphur atom of the thienyl groups S(3), with a Na(1)–S(3) distance of 2.875(2) Å. The Na(2) atoms are coordinated by the three tris(2–thienyl)methanolato ligands and a tetrahydrofuran molecule. The O-Na-O angles within the Na_4O_4 cube are in-between 88.79(8) and 95.45(8)° (Table 5). The overall molecular structure of **8** is quite comparable with those reported for $[Na(\mu_3–Ombp)(DME)]_4$ [23] and $[Na(OC_6H_4Me–4)(dme)]_4$ [24]. In contrast to cage compound **8**, in these latter compounds each metal centre is ligated to a solvent molecule. In our case (see above), only two sodium atoms are surrounded by tetrahydrofuran. Additional intramolecular bonding as in **8** is also observed in the structures of $[Na_4(salphen)_2(dme)_2]$ and $[Na_4(salen)_2(dme)_2]$ [26], where only two of the alkali metals are bonded to the Schiff base, whereas the other two complete their coordination sphere with the oxygen atom of a dme donor. The $Na–OC(C_4H_5S)_3$ bond distances lie in the range found for $[Na(OC_6H_4Me–4)(dme)]_4$ [2.314(0) Å] [24] and $[Na(\mu_3–Ombp)(DME)]_4$ [2.33 Å] [23], although the O-Na-O and Na-O-Na angles are different. These variations of the angles can be explained by the steric difference of the ligands and solvents ligated to the sodium atoms.

Table 5. Selected bond lengths /Å and angles /° for $[NaOC(C_4H_3S)_3]_4(thf)_2$ (**8**).

8			
Na(1)–O(2)	2.323(2)	Na(1)••••Na(1)	3.068(2)
Na(1)–O(1)	2.302(2)	Na(2)••••Na(2)	3.256(2)
Na(2)–O(1)	2.488(2)	Na(1)••••Na(2)	3.290(1)
Na(2)–O(2)	2.286(2)	Na(1)–S(3)	2.875(2)
Na(2)–O(3)	2.325(3)		
Na(1)–O(1)–Na(1)	95.45(8)	O(1)–Na(1)–O(1)	95.45(8)
Na(1)–O(1)–Na(2)	87.00(8)	O(2)–Na(2)–O(2)	88.79(8)
Na(2)–O(2)–Na(2)	91.21(8)	O(2)–Na(1)–O(1)	92.10(8)
Na(2)–O(2)–Na(1)	85.86(8)	C(1)–O(1)–Na(1)	125.1(2)
O(2)–Na(2)–O(1)	93.99(8)	C(14)–O(2)–Na(2)	132.2(2)

Synthesis of the Samarium(III) Thienyl–Substituted Methoxides

The alkaline salts of carbinols **7**-**15** have been used to accede to the samarium derivatives. Three equivalents of the carbinol **1** were deprotonated in the presence of 3 equivalents NaH or KH in tetrahydrofuran at room temperature overnight. Subsequently, the *in situ* formed salts $\{[KOC(C_4H_3S)_3]_4(thf)_2\}$ • thf (**7**) and $\{[NaOC(C_4H_3S)_3]_4(thf)_2\}$ • thf (**8**), respectively were added to a suspension of 1 equivalent of $SmCl_3$ (Scheme 3). After stirring for further three days and work–up, brown–light single crystals of $\{Sm[OC(C_4H_3S)_3]_3(thf)_3\}$ • thf (**16**) were obtained in a modest yield of 24 % and 13 %, respectively. A similar procedure allowed also the synthesis of $\{Sm[OC(C_{16}H_{13}S)]_3(thf)_3\}$ • thf (**17**) by *in situ* deprotonation of carbinol **3** in the presence of KH (Scheme 3). Colourless crystals of have been obtained, albeit in a low yield of only 10 %.

The ^{1}H NMR spectrum of **16**, recorded at room temperature in $CDCl_3$, displays broad signals, probably due to the paramagnetic character of the Sm(III) ion. A broad aromatic signal at 7.2 ppm, which integrates for 27H, is attributed to the protons of the thienyl units. The other signals at 3.4, 1.7, 1.2 and 0.9 ppm are assigned to the different hydrogen atoms of the tetrahydrofuran molecules ligated or not to the metal centre.

The ^{1}H NMR spectrum of **17** exhibits five signals in $CDCl_3$ solution. The first, at 7.3 ppm, is a multiplet, which integrates for 33 H attributed to the protons of the phenyl groups and the 5–H

of the thienyl groups. The two others aromatic signals, doublet of doublets at 6.9 and 6.7 ppm (each integrating for 3H), correspond to the 4–H and 3–H of the thienyl groups, respectively. The hydrogen atoms of tetrahydrofuran are present at 3.7 and 1.8 ppm.

Crystal Structures of the Samarium(III) Thienyl–Substituted Methoxides

Single crystal X–ray structure determinations for compounds **16** and **17**, which crystallize at 5°C from tetrahydrofuran as brown–light or colourless crystals, were performed. Selected bond lengths and angles are gathered in Table 6. Unfortunately, for **17** the differentiation between the thienyl and phenyl groups is difficult due to disorder of the ligands.

Table 6. Selected bond lengths /Å and angles /° for **16** and **17**.

	16	**17**
Sm–O(1)	2.156(3)	2.160(4)
Sm–O(2)	2.594(3)	2.552(5)
O(1)–C(1)	1.391(5)	1.395(8)
O(1)–Sm–O(1)	101.1(1)	102.3(2)
O(1)–Sm–O(2)	92.5(1)	90.8(2)
O(2)–Sm–O(2)	73.7(1)	76.9(2)
C(1)–O(1)–Sm	170.53(6)	173.3(5)

The molecular structures of $\{Sm[OC(C_4H_3S)_3]_3(thf)_3\}$ • thf (**16**) and $\{Sm[OC(C_{16}H_{13}S)]_3(thf)_3\}$ • thf (**17**) exhibit six–coordinate mononuclear samarium alkoxides with three (2–thienyl)methoxido or diphenyl(2–thienyl)methoxido ligands and three tetrahydrofuran molecules around the samarium atoms, in a facial arrangement. Both molecules are situated on a threefold axis in the crystals. Additional thf molecules are filling the crystal lattice with no interaction with the molecules (Figure 6). The overall structures of **16** and **17** is similar to that in $\{Nd[OC(C_4H_3S)_3]_3(thf)_3\}$ • thf [5], $Sm(O–2,4,6–Me_3C_6H_2)(thf)_3$ [20] or $Sm(O–2,6–i–Pr_2C_6H_3)_3(thf)_3$ [19]. The geometry about the samarium centres is distorted octahedrally, as evidence the $(C_4H_3S)_3CO–Sm–OC(C_4H_3S)_3$ [101.1(1)°] or $(C_{16}H_{13}S)OC–Sm–OC(C_{16}H_{13}S)$ [102.3(2)°] and the O(thf)–Sm–O(thf) angles [73.7(1)° for

16 or 76.9(2)° for **17**]. These angle values are comparable with those found for Sm(O–2,6–*i*–$Pr_2C_6H_3)_3(thf)_3$ [102.29(6)° and 79.33(6)°, respectively] [19] or Sm(O–2,4,6–$Me_3C_6H_2)_3(thf)_3$ [103.4(1) and 77.5(1)°, respectively] [20]. The Sm–O–C$(C_4H_3S)_3$ angles of 170.5(3)° and Sm–O–C$(C_{16}H_{13}S)$ of angles of 173.3(5)° are also similar to those in {Nd[OC$(C_4H_3S)_3]_3(thf)_3$} • thf [169.9(1)°] [5] and in Sm(O–2,4,6–$Me_3C_6H_2)_3(thf)_3$ [170.0(3)°] [20]. The Sm–OC$(C_4H_3S)_3$ and Sm–OC$(C_{16}H_{13}S)$ distances of 2.156(3) and 2.160(4) Å are comparable to those in Sm(O–2,4,6–$Me_3C_6H_2)_3(thf)_3$ [2.160(0) Å] [20], Sm(O–2,6–*i*–$Pr_2C_6H_3)_3(thf)_3$ [2.158(2) Å] [19] and [Sm($OC_6H_2Bu^t_2$–2,6–Me–4)$_3$(thf)] • thf [2.152(7) Å] [27]. The Sm–O(thf) distances are longer with 2.594(3) Å (**16**) and 2.552(5) Å (**17**) and are in the range of those observed for Sm(O–2,6–*i*–$Pr_2C_6H_3)_3(thf)_3$ [2.542(2) Å] [19]. These distances are also in accordance with those found for the compound {Nd[OC$(C_4H_3S)_3]_3(thf)_3$} • thf [5].

Electrochemical Studies

The electrochemical investigations of thiophenes and its derivatives is a classical technique to study the physico–chemical properties of thienyl compounds [28]. Since the last decade, the incorporation of transition metals or rare earths metal centres into the thiophene derivatives has emerged as interesting extensions, thus combining the intrinsic properties of metal ions with those of thienyl–based heterocycles [29–31]. It is well known that the most stable oxidation state of the lanthanide elements is +3 [32], but the oxidation state +2 is also well–established, in particular for the samarium ion [33]. Nevertheless the value of the Sm^{3+}/Sm^{2+} potential depends to the environment around the metal [34]. In this context, we investigated the electrochemical properties of the carbinols **1**–**6**, those of their derived alkali metal alcoholates **7**–**15** and of the samarium alkoxides **16**–**17**.

Carbinols and Alkali Metal Alcoholates

The values of peak potentials of carbinols **1**–**6** and the samarium alkoxides **16** and **17** obtained in acetonitrile are listed in Table 7.

Table 7. Values peak potentials [V, vs. $Ag/AgClO_4$] of the carbinols and their alkali metal derivatives, in acetonitrile (10^{-3} M or 2×10^{-3} for **5**, **14**, **6** and **15**) deduced from cyclic voltammetric measurements on a platinum electrode (diameter 1 mm), scan rate 100 $mV.s^{-1}$.

	E_{pa} [V]	E_{pc} [V]
$HO–C(C_4H_3S)_3$ (**1**)	1.54	–0.12
$\{[KOC(C_4H_3S)_3]_4(thf)_2\}$ • thf (**7**)	1.53	–
$[NaOC(C_4H_3S)_3]_4(thf)_2$ (**8**)	1.47	–0.13
$HO–C(C_{14}H_{11}S_2)$ (**2**)	1.50	–0.16
$[KOC(C_{14}H_{11}S_2)]_4(thf)_3$ (**9**)	1.41	–0.18
$[NaOC(C_{14}H_{11}S_2)]_4(thf)_2$ (**10**)	1.42	–
$HO–C(C_{16}H_{13}S)$ (**3**)	1.55	–0.11
$\{[KOC(C_{16}H_{13}S)]_4(thf)_3\}$ • ½ thf (**11**)	1.50	–0.14
$HO–C(C_{17}H_{15}S)$ (**4**)	1.39	–
$[KOC(C_{17}H_{15}S)]_4(thf)_2$ (**12**)	1.30	–
$[NaOC(C_{17}H_{15}S)]_4(thf)_2$ (**13**)	1.29	–0.27
$HO–C(C_{14}H_{11}S_2)$ (**5**)	1.62	–
$[NaOC(C_{14}H_{11}S_2)]_4(thf)_2$ (**14**)	1.67	–0.21
$HO–C(C_{16}H_{13}S)$ (**6**)	1.77	–
$[NaOC(C_{16}H_{13}S)]_4(thf)_2$ (**15**)	1.76	–0.17

The voltammograms of **1**–**3** between –0.50 and +2.00 V vs. $Ag/AgClO_4$ on a platinum electrode at 100 $mV.s^{-1}$ lead to two irreversible signals (for example see Figure 7). The first wave is assigned to the oxidation of the thienyl units [35]. The second waves correspond to the reduction of the carbocation. Indeed, during the oxidation of the thienyl units, some H^+ are formed and can deprotonate the carbinols leading to a stable carbocation [6, 36]. The voltammograms of **5** and **6** depict only the irreversible wave due to the oxidation of the thienyl groups, at 1.62 V and 1.77 V, respectively. Note that, in comparison with **3**, the oxidation peak potential of **4** is shifted towards lower values (1.55 V for **3**, 1.39 V for **4**): the introduction of an electron donating methyl group facilitates the oxidation process manifested by a decrease of the potential [37]. The values of the oxidation peak potentials of **5** and **6** are

higher than those obtained for **2** and **3**. This is probably due to the fact that, contrarily to **2** and **3**, the two alpha positions of the thienyl units are unsubstituted [28h]. By repetitive cyclic voltammetry of the carbinols, no formation of polymeric films is evidenced. This failure may be explained by the high reactivity of the cation radicals generated, which can react with a molecule of solvent or undergo nucleophilic attack. These results are in good agreement with observations performed on other molecules with an unsubstituted α–position on pyrroles [38].

The voltammograms of the alkali metal alcoholates **7**–**15** (for example see Figure 8) show an oxidation irreversible wave due to the oxidation of the thiophene moieties. For **8**–**9**, **11** and **13**–**15**, a second wave is observed on the cyclic voltammogram from –0.13 to –0.27 V and corresponding to the reduction of the carbocation generated during the process (see above). Nevertheless, for the compounds **7**, **10** and **12**, the lifetime of the carbocation formed during the oxidation is not long enough to be reduced. No polymeric film is formed during the oxidation process: this result matches with the findings obtained for the respective ligands. In comparison with the corresponding carbinol, the oxidation peak potentials are shifted towards lower values by 0.01–0.10 V, probably due to the inductive effect of the alkali metal which increases the electronic density of the thiophene moieties leading to an easier oxidation of this species or to the change in the interannular conjugation within the structure of the metal alcoholates [39]. Nevertheless, this observation has not been made for the sodium alcoholate **14**: in this case the oxidation peak potential is shifted towards an incomprehensible higher value (1.62 V for **5** and 1.67 V for **14**).

As can be seen, the number of thienyl units has no significant effect on the electrochemical properties of the compounds whereas the functionalization of these groups (see **3** compared to **4**) or their different attached positions have an influence on the oxidation values (see for example **5/6** compared to **2/3**).

Samarium alkoxides

The values of peak potentials of carbinols **1** and **3** and the samarium alkoxides **16** and **17** obtained in dichloromethane are listed in Table 8 (the measurements in acetonitrile are not possible due to the insolubility of the lanthanide alkoxides).

Table 8. Values peak potentials [V, vs. $Ag/AgClO_4$] of the carbinols **1** and **3** and samarium alkoxides **16** and **17**, in dichloromethane deduced from cyclic voltammetric measurements (0 → –1.5 → 1.5 → 0 V) on a platinum electrode (diameter 1 mm) at 100 $mV.s^{-1}$.

	E_{pa} [V]
$HO–C(C_4H_3S)_3$ (**1**)	1.48
$\{Sm[OC(C_4H_3S)_3]_3(thf)_3\}$ • thf (**16**)	1.62
$HO–C(C_4H_3S)_3$ (**3**)	1.64
$\{Sm[OC(C_{16}H_{13}S)]_3(thf)_3\}$ • thf (**17**)	1.56

The voltammograms exhibit only one irreversible wave at 1.62 V for **16** and at 1.56 V for **17** (Figure 9) attributed to the oxidation of the thienyl moieties [35]. When potentials are cycles, no reduction of samarium(III) to samarium(II) is visible at about –0.8 V [34, 40]. To explain this observation several hypotheses are possible: i) the electron–rich organic ligands make a more difficult electron transfer to the lanthanide ion shifting the reduction potential of the samarium towards high negative values [34] which are not detectable in the common electrochemical solvent, ii) the samarium metal centre is wrapped up by the electron–rich organic ligands leading to the inhibition of the reduction process and to the stabilisation of the metal centre.

Luminescence Studies

Recently, several studies have demonstrated that thiophene–derived ligand systems can be promising candidates as sensitizing chromophore in lanthanide compounds [41, 42]. In these conjugated coordination compounds, the ligand acts as donor and the lanthanide ion as acceptor. But in our compounds, the conjugation is interrupted by the methoxido group and also no π–interaction between the thienyl and/or phenyl units can be assumed in the solid state (spatial distance from the aromatic groups to the metal: ~ 5 Å). Therefore, it was intriguing to study, if, under these conditions, an antenna effect is still present.

The carbinols and the alkali metal alcoholates were investigated in comparison to the samarium compounds, as well to get some insight in the ligand absorptions and emissions.

Carbinols and Alkali Metal Alcoholates

The solid–state emission maxima of the tertiary alcohols **1**–**6** and their derived alkali metal alcoholates **7**–1**5** are given in Table 9.

Table 9. Solid−state emission maxima λ_{em} [nm] of the carbinols and the alkali metal alkoxides (K, Na) with λ_{ex} for excitation maximum.

	λ_{em} [nm]
HO–C(C_4H_3S)$_3$ (**1**)	430 (λ_{ex} = 280 nm)
{[KOC(C_4H_3S)$_3$]$_4$(thf)$_2$} • thf (**7**)	390 (λ_{ex} = 240 nm)
[NaOC(C_4H_3S)$_3$]$_4$(thf)$_2$ (**8**)	393 (λ_{ex} = 240 nm)
HO–C($C_{14}H_{11}S_2$) (**2**)	402 (λ_{ex} = 260 nm)
[KOC($C_{14}H_{11}S_2$)]$_4$(thf)$_3$ (**9**)	396 (λ_{ex} = 250 nm)
[NaOC($C_{14}H_{11}S_2$)]$_4$(thf)$_2$ (**10**)	408 (λ_{ex} = 360 nm)
HO–C($C_{16}H_{13}S$) (**3**)	392 (λ_{ex} = 310 nm)
{[KOC($C_{16}H_{13}S$)]$_4$(thf)$_3$} • ½ thf (**11**)	385 (λ_{ex} = 310 nm)
HO–C($C_{17}H_{15}S$) (**4**)	527 (λ_{ex} = 360 nm)
[KOC($C_{17}H_{15}S$)]$_4$(thf)$_2$ (**12**)	486 (λ_{ex} = 390 nm)
[NaOC($C_{17}H_{15}S$)]$_4$(thf)$_2$ (**13**)	430 (λ_{ex} = 340 nm)
HO–C($C_{14}H_{11}S_2$) (**5**)	400 (λ_{ex} = 260 nm)
[NaOC($C_{14}H_{11}S_2$)]$_4$(thf)$_2$ (**14**)	398 (λ_{ex} = 260 nm)
HO–C($C_{16}H_{13}S$) (**6**)	398 (λ_{ex} = 260 nm)
[NaOC($C_{16}H_{13}S$)]$_4$(thf)$_2$ (**15**)	397 (λ_{ex} = 260 nm)

All the emission spectra are very similar and consist of broad, nearly Gaussian shaped bands with nearly identical maxima which are attributed to the $\pi^* \rightarrow \pi$ transitions of the aromatic units [43]. The carbinol ligands **1**, **2** and **3** [6] fluoresce quite strongly in solid−state, with the peak of the emission band shifting toward lower energy with increasing number of thienyl units (Figure 10). Furthermore, it is worth pointing out that grafting a methyl group in position 5 of thienyl unit generates a red shift of $\Delta\lambda_{em}$ ~ 135 nm for ligand **4** compared to ligand **3** (Figure 10), which significantly decreases the energy level of the LUMO orbital [30]. On the other hand, ligands **5** and **6** exhibit emission maxima in similar range comparing with **2** and **3**, respectively.

For the alkali metal alcoholates, blue shifts of the emission maxima compared to those of the thiophenic alcohols are observed (excepted for **10**). In general, this shift of the transitions compared to those of the thiophenic alcohols is due to some distortions of these units when bonded to potassium or sodium metals [85]. Note that the number of thienyl units, their attached positions or their functionalization have the same effect on the luminescence properties as those observed for their corresponding carbinols.

Samarium Alkoxides

The room temperature emission spectrum of **16** (Figure 11) upon an excitation on the organic ligand (λ_{ex} = 270 nm, see above) displays the typical Sm^{3+} bands at around 570, 604, 650 nm. They are attributed to $4f^5$–$4f^5$ transitions $^4G_{5/2} \rightarrow {}^6H_{5/2}$ (zero–zero band: forbidden transition), $^4G_{5/2} \rightarrow {}^6H_{7/2}$ (magnetic dipole transition), $^4G_{5/2} \rightarrow {}^6H_{9/2}$ (electric dipole transition), respectively [9b, 9c, 9i]. Note that another samarium band at 622 nm is observed, probably also due to the $^4G_{5/2} \rightarrow {}^6H_{7/2}$ transition: it might be a result of splitting due to ligand field. The intense spectrum is typical for an "antenna effect", resulting in an energy transfer from the ligand to the lanthanide centre [45]. Nevertheless, in addition of the Sm^{3+} emission, a broad band is assigned to the fluorescence from the organic ligand in the range from 350 to 520 nm. The relative intensity between the broad band and the Sm^{3+} emission lines suggests that the efficiency of the energy transfer ligand–to–metal process (probably a dipole–dipole energy transfer mechanism) does not seem to be maximal.

The emission spectrum of **17,** when the $^4F_{7/2}$ level (410 nm) is excited (Figure 12), is composed of a series of straight lines assigned to the Sm^{3+} intra–$4f^5$ transitions: $^4G_{5/2} \rightarrow {}^6H_{5/2,7/2,9/2}$. Note that, as **16**, a samarium band at 622 nm is observed, probably also due to the $^4G_{5/2} \rightarrow {}^6H_{7/2}$ transition: it might be a result of splitting due to ligand field.

The solid–state excitation spectra of **16** and **17** monitoring the $^4G_{5/2} \rightarrow {}^6H_{9/2}$ transition recorded at room temperature are given in Figure 13. They show broad bands that cover the entire 250–300 nm region with a maximum at 270 nm for **16** and the 250–395 nm region with a maximum at 273 for **17** attributed to the $\pi \rightarrow \pi^*$ transitions of the organic ligands. The spectra also present several narrow bands of the Sm^{3+} ion arising from the intraconfigurational transitions from the $^6H_{5/2}$ ground state to the following levels: $^4H_{9/2}$ (~ 344 nm), $^4F_{9/2}$ (~ 363

nm), $^4L_{17/2}$ (~ 373 nm), $^4F_{7/2}$ (~ 406 nm), (^6P, $^4P)_{5/2}$ (~ 422 nm), $^4G_{9/2}$ (~ 450 nm), $^4I_{13/2}$ (~ 462 nm), $^4I_{11/2}$ (~ 473 nm), $^4I_{9/2}$ (~ 488 nm), $^4G_{7/2}$ (~ 504 nm), $^4F_{3/2}$ (~ 526 nm) and $^4G_{5/2}$ (~ 568 nm). These transition values are in agreement with those found for Sm^{3+} doped germinate glasses and glass ceramic and those for samarium complexes [8, 42].

Conclusion

A series of novel potassium and sodium carbinolates containing thienyl substituents have been obtained and their crystal structures investigated. The molecular structures exhibit only distorted cubane–like M_4O_4 cores. Each alkali metal is surrounded by three carbinolato ligands and two or three alkali ions are additionally ligated with a tetrahydrofuran molecule. In addition, two new samarium(III) methoxides containing thienyl substituents have been synthesized and structurally characterized. Their X–ray structures reveal only mononuclear molecules with an octahedral coordination sphere around the metal centre in a facial ligand arrangement. The physico–chemical studies of the series of alkali metal alcoholates or samarium alkoxides containing thienyl substituents have shown that their electrochemical properties are only dominated by organic ligands. The emission spectra of the carbinols and potassium or sodium alcoholates depict broad bands attributed to the aromatic groups. Nevertheless, the luminescence spectra of the Sm^{3+} alkoxides exhibit an energy transfer from the ligand to the lanthanide centre.

To compare the influence of the samarium oxidation state on the crystal structure, electrochemical and luminescence properties of samarium alkoxides bearing thienyl moieties, the study of the reactivity of our alkali metal alcoholates towards SmX_2 (X = Cl, I) is in progress. Furthermore, some experiments with other rare earths such as Eu^{3+}, Tb^{3+}, Pr^{3+} and /or with other thiophenes derivatives are underway.

Acknowledgments

We gratefully acknowledge the financial support provided by the DFG in the framework of the SPP1166 (Lanthanoidspezifische Funktionalitäten in Molekül und Material), by the Saarland University and the Fonds der Chemischen Industrie. We thank Dr. Michael Zimmer for the ^1H NMR spectra of **16** and **17**. MK and LG thank the CNRS for financial support.

References

[1] a) I. A. Hemmilä, *Application of Fluorescence in Immunoassay*s, Wiley, New York, **1991**; b) J.–C. G. Bünzli, G. R. Choppin, (Eds.), *Lanthanide Probes in Life, Chemical and Eart Science – Theory and Pratice*, Elsevier, Amsterdam, **1989**; c) R. Reyes, E. N. Hering, M. Cremona, C. F. B. Silva, H. F. Brito, C. A. Achete, *Thin Solid Films* **2002**, *420–421*, 23–29.

[2] N. Sabatini, M. Guardigli, J. M. Lehn, *Coord. Chem. Rev.* **1993**, *123*, 201–228.

[3] a) B. Yan, H. J. Zhang, S. B. Wang, J. Z. Ni, *Spectrosc. Lett.* **1998**, *31*, 603–613; b) S. Sato, M. Wada, *Bull. Chem. Jpn.* **1970**, *43*, 1955–1962.

[4] a) H. C. Aspinall, S. A. Cunningham, *Inorg. Chem.* **1998**, *37*, 5396–5398, b) B. Cetinkaya, P. B. Hitchcock, M. F. Lappert, R. G. Smith, *J. Chem. Soc, Chem. Commun.* **1992**, 932–934; c) M. Niemeyer, *Eur. J. Inorg. Chem.* **2001**, 1969–1981; d) S. M. Cendrowski–Guillaume, G. L. Gland, M. Nierlich, M. Ephritikhine, *Organometallics* **2000**, *19*, 5654–5660; e) J. H. Melman, T. J. Emge, J. G. Brennan, *Chem. Commun.* **1997**, 2269–2270; f) J. Lee, D. Freedman, J. H. Melman, M. Brewer, L. Sun, T. J. Emge, F. H. Log, J. G. Brennan, *Inorg. Chem.* **1998**, *37*, 2512–2519; g) S. Banerjee, T. J. Emge, J. G. Brennan, *Inorg. Chem.* **2004**, *43*, 6307–6312; h) K. Mashima, T. Shibahara, Y. Nakayama, A. Nakamura, *J. Organomet. Chem.* **1998**, *559*, 197–209.

[5] M. Veith, C. Belot, L. Guyard, V. Huch, M. Knorr, M. Zimmer, *Eur. J. Inorg. Chem.* **2008**, 2397–2406.

[6] M. Veith, C. Belot, V. Huch, H.–L. Cui, L. Guyard, M. Knorr, C. Wickleder, *Eur. J. Inorg. Chem.* **2010**, 879–889.

[7] a) W. S. Hwang, D. L. Wang, M. Y. Chiang, *J. Organomet. Chem.* **2000**, *613*, 231–235; b) Y. F. Tzeng, C. Y. Wu, W. S. Hwang, C. H. Hung, *J. Organomet. Chem.* **2003**, *687*, 16–26; c) J. Lloret, F. Estevan, P. Lahuerta, P. Hirva, J. Pérez–Prieto, M. Sanaù, *Organometallics* **2006**, *25*, 3156–3165; d) D. Wang, D. Cui, W. Miao, S. Li, B. Huang, *Dalton Trans.* **2007**, 4576–4591.

[8] G. Lakshminarayana, H. Yang, Y. Teng, J. J. Qui, *Lum.* **2009**, *129*, 59–68.

[9] a) Y. Hasegawa, S.–I. Tsuruoka, T. Yoshida, H. Kawai, T. Kawai, *J. Phys. Chem. A* **2008**, *112*, 803–807; b) M. D. Regulacio, M. H. Pablico, J. Acay Vasquez, P. N. Myers, S. Gentry, M. Prushan, S.–W. Tam–Chang, S. L. Stoll, *Inorg. Chem.* **2008**, *47*, 1512–1523; c) Y. Hasegawa, S.–I. Tsuruoka, T. Yoshida, H. Kawai, T. Kawai, *J. Phys. Chem. A* **2008**, 112, 803–807; d) J. Fang, H. You, J. Chen, J. Lin, D. Ma, *Inorg. Chem.* **2006**, *45*, 3701–3704; e) A. P. Bassett, S.

W. Magennis, P. B. Glover, D. J. Lewis, N. Spencer, S. Parsons, R. M. William, L. De Cola, Z. Pikramenou, *J. Am. Chem. Soc.* **2004**, *126*, 9413–9424; f) S. Quici, M. Cavazzini, G. Accosi, N. Armaroli, B. Vantura, F. Barigelleti, *Inorg. Chem.* **2005**, *44*, 529–537; g) H. Brito, O. L. Malta, M. C. F. C. Felinto, E. E. S. Teotonio, J. F. S. Menezes, C. F. B. Silva, C. S. Tomiyama, C. A. A. Carvalho, *J. Alloys Compd.* **2002**, *344*, 293–297; h) S. Petoud, S. M. Cohen, J.–C. G. Bünzli, K. N. Raymond, *J. Am. Chem. Soc.* **2003**, *125*, 13324–13325; i) P. C. R. Soares–Santos, H. I. S. Nogueria, F. A. Almeida Paz, R. A. Sá Ferreira, L. D. Carlos, J. Klinowski, T. Trindade, *Eur. J. Inorg. Chem.* **2003**, *19*, 3609–3617; j) B.–L. An, M.–L. Gong, M.–X. Li, J.–M. Zhang, *J. Mol. Struct.* **2004**, *687*, 1–6; k) B. Yan, Q. Wie, *J. Mol. Struct.* **2004**, *688*, 73–78.

[10] H. Paulsen, S. Antons, A. Brandes, M. Logers, S.N. Muller, P. Naab, C. Schmeck, S. Schneider, J. Stoltefuss, *Angew. Chem. Int. Ed.* **1999**, *38*, 3373–3375.

[11] A. Lebrun, J.–L. Namy, H. B. Kagan, *Tetrahedron Lett.* **1991**, *32*, 2355–2358.

[12] P. Van de Weghe, J. Collin, *Tetrahedron Lett.* **1994**, *35*, 2545–2548.

[13] D. A. Evans, A. H. Hoveyda, *J. Am. Chem. Soc.* **1990**, *112*, 6447–6449.

[14] K. Katagiri, M. Kameoka, M. Nishiura, T. Imamoto, *Chem. Lett*. **2002**, *31*, 426–427.

[15] B. Abarca, G. Asencio, R. Ballesteros, T. Varea, *J. Org. Chem*. **1991**, *56*, 3224–3229.

[16] G. M. Sheldrick, *Acta Cryst*. **2008**, *A64*, 112-122.

[17] Diamond, Crystal and Molecular Structure Visualization. CRYSTAL IMPACT, Postfach 1251, 53002 Bonn, Germany. (www.crystalimpact.com/diamond/).]

[18] S. Sankhla, R. N. Kapoor, *Austr. J. Chem.* **1967**, *20*, 2013–2016.

[19] Z. Xie, K. Chui, Q. Yang, T. C. W. Mak, J. Sun, *Organometallics* **1998**, *17*, 3937–3944.

[20] G. R. Giesbrecht, J. C. Gordon, D. L. Clark, B. L. Scott, J. G. Watkin, K. J. Young, *Inorg. Chem.* **2002**, *41*, 6372–6379.

[21] a) Y.–M. Yao, Q. Shen, Y. Zhang, M.–Q. Xue, J. Sun, *Polyhedron* **2001**, *20*, 3201–3208; b) L.–L. Zhang, Y.–M. Yao, Y.–J. Luo, Q. Shen, J. Sun, *Polyhedron* **2000**, *19*, 2243–2247; c) J. Gromada, A. Moretux, T. Chenal, J. W. Ziller, F. Leising, J.–F. Carpentier, *Chem. Eur. J.* **2002**, *8*, 3773–3788; d) W. J. Evans, M. S. Sollberger, T. P. Hanusa, *J. Am. Chem. Soc.* **1988**, *110*, 1841–1850; e) W. J. Evans, M. S. Sollberger, *Inorg. Chem.* **1988**, *27*, 4417–4423; f) W. J. Evans, M. A. Ansari, J. W. Ziller, S. I. Khan, *J. Organomet. Chem.* **1998**, *553*, 141–148; g) D. L. Clark, J. C. Gordon, J. G. Watkin, *Polyhedron* **1996** , *15*, 2279–2289.

[22] a) D. Walther, U. Ritter, S. Geβler, J. Sieler, M. Kurnert, *Z. Anorg. Allg. Chem.* **1994**, *620*, 101–106; b) M. B. Dinger, M. J. Scott, *Inorg. Chem.* **2000**, *39*, 1238–1254; c) D. J. MacDougall, B. C. Noll, K. W. Henderson, *Inorg. Chem.* **2005**, *44*, 1181–1183; d) J. A.

Samuels, E. B. Lobkovsky, W. E. Streib, K. Folting, J. C. Huffman, J. W. Zwanziger, K. G. Caulton, *J. Am. Chem. Soc.* **1993**, *115*, 5013–5104; e) P. Sobota, M. Klimowicz, J. Utko, L. B. Jerzykiewicz, *New J. Chem.* **2000**, *24*, 523–526; f) G. Müller, T. Schätzle, *Z. Naturforsch.* **2004**, *59b*, 1400–1410; g) P. A. van der Schaaf, J. T. B. H. Jastrzebski, M. P. Hogerheide, W. J. J. Smeets, A. L. Spek, J. Boersma, G. van Koten, *Inorg. Chem.* **1993**, *32*, 4111–4118; h) J. Geier, H. Rüegger, H. Grützmacher, *Dalton Trans.* **2006**, 129–136; i) M. B. Dinger, M. J. Scott, *Chem. Commun.* **1999**, 2525–2526.

[23] M. L. Cole, P. C. Junk, K. M. Proctor, J. L. Scott, C. R. Strauss, *Dalton Trans.* **2006**, 3338–3349.

[24] W. J. Evans, R. E. Golden, J. W. Ziller, *Inorg. Chem.* **1993**, *32*, 3041–3051.

[25] T. J. Boyle, N. L. Andrews, M. A. Rodriguez, C. Campana, T. Yiu, *Inorg. Chem.* **2003**, *42*, 5357–5366.

[26] E. Solari, S. De Angelis, C. Floriani, A. Chiesi, C. Rizzoli, *J. Chem. Soc. Dalton Trans* **1991**, 2471.

[27] G. Qi, Y. Lin, J. Hu, Q. Shen, *Polyhedron* **1995**, *14*, No 3, 413–415.

[28] a) S. J. Howell, C. S. Day, R. E. Noftle, *Inorg. Chim. Acta* **2005**, *358*, 3711–3723; b) J. Dai, C. S. Day, R. E. Noftle, *Tetrahedron* **2003**, *59*, 9389–9397; c) A. Jouait, A. Al Badri, M. Goeffroy, G. Bernardinelli, *J. Organomet. Chem.* **1997**, *529*, 143–149; d) F. Sundholm, G. Sundholm, M. Törrönen, *Synth. Met.* **1992**, *53*, 109–114; e) F. Ç. Cebeci, H. Geyik, E. Sezer, A. S. Sarac, *J. Electroanal. Chem.* **2007**, *610*, 113–121; f) A. Almutairy, F. S. Tham, M. J. Marsella, *Tetrahedron* **2004**, *60*, 7187–7190; g) L. Guyard, M. Nguyen Dinh An, P. Audebert, *Adv. Mater.* **2001**, *13*, 133–136; h) F. Chérioux, L. Guyard, *Adv. Funct. Mater.* **2001**, *11*, 305–309; i) G. Zotti, B. Vercelli, A. Berlin, S. Destri, M. Pasini, V. Hernández, J. T. López Navarrete, *Chem. Mater.* **2008**, *20*, 6847–6856.

[29] a) K. R. Justin Thomas, J. T. Lin, *J. Organomet. Chem.* **2001**, *637–639*, 139–144; b) D. Obendorf, H. Schottenberger, K. Wurst, N. Schuler, G. Laus, *J. Organomet. Chem.* **2005**, 811–817; c) A. Arnanz, M.–L. Marcos, S. Delgado, J. González–Velasco, C. Moreno, *J. Organomet. Chem.* **2008**, *693*, 3457–3470; d) M. O. Wolf, M. S. Wrighton, *Chem. Mater.* **1994**, *6*, 1526–1533; e) T. L. Stott, M. O. Wolf, *Coord. Chem. Rev.* **2003**, *246*, 89–101.

[30] M. Beley, D. Delabouglisse, G. Houppy, J. Husson, J.–P. Petit, *Inorg. Chim. Acta* **2005**, *358*, 3075–3083.

[31] R. Sultan, K. Gadamsetti, S. Swavey, *Inorg. Chim. Acta* **2006**, *359*, 1233–1238.

[32] F. A. Cotton, G. Wilkinson, *Advanced Inorganic Chemistry*, 4th. Ed, Wiley: New York, 1980, Chapter 23.

[33] D. A. Johnson, *J. Chem. Soc. Dalton Trans.* **1974**, 1671–1675.

[34] A. M. Bond, G. B. Deacon, R. H. Newnham, *Organometallics* **1986**, *5*, 2312–2316.

[35] M. Turbiez, P. Frère, M. Allain, N. Gallego–Planas, J. Roncali, *Macromolecules* **2005**, *38*, 6806–6812.

[36] C. Belot, C. Filiatre, L. Guyard, A. Foissy, M. Knorr, *Electrochem. Commun.* **2005**, *7*, 1439–1444.

[37] O. Clot, M. O. Wolf, B. O. Patrick, *J. Am. Chem. Soc.* **2001**, *123*, 9963–9973.

[38] a) C. P. Andrieux, P. Hapiot, P. Audebert, L. Guyard, M. Nguyen Dinh An, L. Groenendaal, E. W. Meijer, *Chem. Mater.* **1997**, *9*, 723–729; b) L. Guyard, P. Hapiot, P. Neta, *J. Phys. Chem. B* **1997**, *101*, 5698–5706; c) P. Garcia, J.–M. Pernaut, P. Hapiot, V. Wintgens, P. Valat, F. Garnier, D. Delabouglise, *J. Phys. Chem.* **1993**, *97*, 513–516; d) P. Bäuerle, U. Segelbacher, A. Maier, M. Mehring, *J. Am. Chem. Soc*. **1993**, *115*, 10217–10223; e) P. Hapiot, F. Demanze, A. Yassar, F. Garnier, *J. Phys, Chem.* **1996**, *100*, 8397–8401.

[39] O. Clot, Y. Akahori, C. Moorlag, D. B. Leznoff, M. O. Wolf, B. O. Patrick, M. Ishii, *Inorg. Chem.* **2003**, *42*, 2704–2713.

[40] A. I. Bhatt, I. May, V. A. Volkovich, D. Collison, M. Helliwell, I. B. Polovov, R. G. Lewin, *Inorg. Chem.* **2005**, *44*, 4934–4940.

[41] a) Y.–F. Yuan, T. Cardinaels, K. Lunstroot, K. Van Hecke, L. Van Meervelt, C. Görller–Walrand, K. Binnemans, P. Nockemann, *Inorg. Chem.* **2007**, *46*, 5302–5309; b) S. Viswanathan, A. de Bettencourt–Dias, *Inorg. Chem.* **2006**, *45*, 10138–10146; c) de A. Bettencourt–Dias, S. Viswanathan, A. Rollet, *J. Am. Chem. Soc.* **2007**, *129*, 15436–15437.

[42] E. E. S. Teotonio, M. C. F. C. Felinto, H. F. Brito, O. L. Malta, A. C. Trindade, R. Najjar, W. Strek, *Inorg. Chim. Acta* **2004**, *357*, 451–460.

[43] R. S. Becker, J. Seixa de Melo, A. L. Maçanita, F. Elisei, *J. Phys. Chem.* **1996**, *100*, 18683–18695.

[44] P. C. R. Soares–Santos, F. A. Almeida Paz, R. A. Sá Ferreira, J. Klinowski, L. D. Carlos, T. Trindade, H. I. S. Nogueira, *Polyhedron* **2006**, *25*, 2471–2482.

[45] J.–C. Bünzli, *J. Alloys Compd.* **2006**, *408–412*, 934–944.

Figure captions

Anmerkung an die Redaktion: Bitte unter die gegliederten Abbildungen (2 bis 6) die Zuordnungen in der Bildunterschrift jeweils in einer Textzeile wie folgt einfügen:

Abb. 2, 3 und 5:a) unter die linke, b) unter die rechte Abbildung
Abb. 4: 9 nach links, 12 nach rechts
Abb. 6: 16 nach links, 17 nach rechts

Die Zuordnungen sind durch die separate Einreichung der Abbildungen und Bildunterschriften leider verloren gegangen.

Vielen Dank!

Figure 1. Overview of carbinols **1**–**6** used as starting materials.

Figure 2. a) ORTEP (30 % ellipsoid) representation of $\{[KOC(C_4H_3S)_3]_4(thf)_2\} \bullet thf$ (**7**). The carbon atoms of the heterocycles are depicted as sticks. The hydrogen atoms and the lattice thf molecule are omitted for more clarity. Two thienyl groups are found in two split positions [S(1A) and S(1B), S(2A) and S(2B)]. B) View of the distorted heterocubane core.

Figure 3. a) ORTEP (30 % ellipsoid) representation of $\{[KOC(C_{16}H_{13}S)]_4(thf)_3\} \bullet ½\ thf$ (**11**). The carbon atoms of the phenyl and thienyl groups are depicted as sticks. The hydrogen atoms and the lattice tetrahydrofuran molecule are omitted for more clarity. b) View of the distorted heterocubane core.

Figure 4. ORTEP (30 % ellipsoid) representation of $[KOC(C_{14}H_{11}S_2)]_4(thf)_3$ (**9**) and $[KOC(C_{17}H_{15}S)]_4(thf)_2$ (**12**). The carbon atoms of the aromatic groups are depicted as sticks. The hydrogen atoms and the lattice tetrahydrofuran molecule are omitted for more clarity.

Figure 5. a) ORTEP (30 % ellipsoid) representation of $[NaOC(C_4H_3S)_3]_4(thf)_2$ (**8**). Hydrogen atoms are omitted for more clarity. b) Environment around the sodium atoms.

Figure 6. ORTEP (30 % ellipsoid) representation of $\{Sm[OC(C_4H_3S)_3]_3(thf)_3\}$ • thf (**16**) and $\{Sm[OC(C_{16}H_{13}S)]_3(thf)_3\}$ • thf (**17**). The tetrahydrofuran lattice molecule and hydrogen atoms are omitted for more clarity. For **16**, one type of disordered carbon atoms of the heterocycles is depicted as sticks. For **17**, the thienyl and phenyl units are found in different positions [S(1) and S(2)].

Figure 7. Cyclic voltammogram recorded on a platinum electrode (diameter 1 mm) in an acetonitrile solution containing $HO–C(C_4H_3S)_3$ (**1**) (10^{-3} M) and $[NBu_4][PF_6]$ (0.1 M), vs. $Ag/AgClO_4$, at 100 $mV.s^{-1}$.

Figure 8. Cyclic voltammograms recorded on a platinum electrode (diameter 1 mm) in an acetonitrile solution $[NaOC(C_4H_3S)_3]_4(thf)_2$ (**8**) (10^{-3} M) and $[NBu_4][PF_6]$ (0.1 M), vs. $Ag/AgClO_4$, scan rate 100 $mV.s^{-1}$.

Figure 9. Cyclic voltammogramm recorded at a platinum electrode on a dichloromethane solution containing **17** (3.32×10^{-3} M) and $[NBu_4][PF_6]$ (0.1 M), vs. $Ag/AgClO_4$, scan rate 100 $mV.s^{-1}$, between $0 \rightarrow -1.5 \rightarrow 2$ and 0 V.

Figure 10. Room temperature solid–state luminescence spectra. Centre: **1** (λ_{ex} = 280 nm), dash line: **2** (λ_{ex} = 260 nm), left: **3** (λ_{ex} = 310 nm) and right: **4** (λ_{ex} = 360 nm).

Figure 11. Solid–state emission spectrum at room temperature for compound **16**, λ_{ex} = 270 nm.

Figure 12. Solid–state emission spectrum at room temperature for compound **17**, λ_{ex} = 410 nm.

Figure 13. Solid−state excitation spectrum at room temperature for compound $\{Sm[OC(C_4H_3S)_3]_3(thf)_3\}$ • thf (**16**) (solid line) and $\{Sm[OC(C_{16}H_{13}S)]_3(thf)_3\}$ • thf (**17**) (dashed line), λ_{em} = 651 and 650 nm, respectively.

Scheme 1. Synthesis of HO−C($C_{17}H_{15}S$) (**4**).

Scheme 2. General route of potassium or sodium alcoholates **7**–**15**.

Scheme 3. Salt−elimination route leading to Sm(III) thienyl−functionalized methoxides.

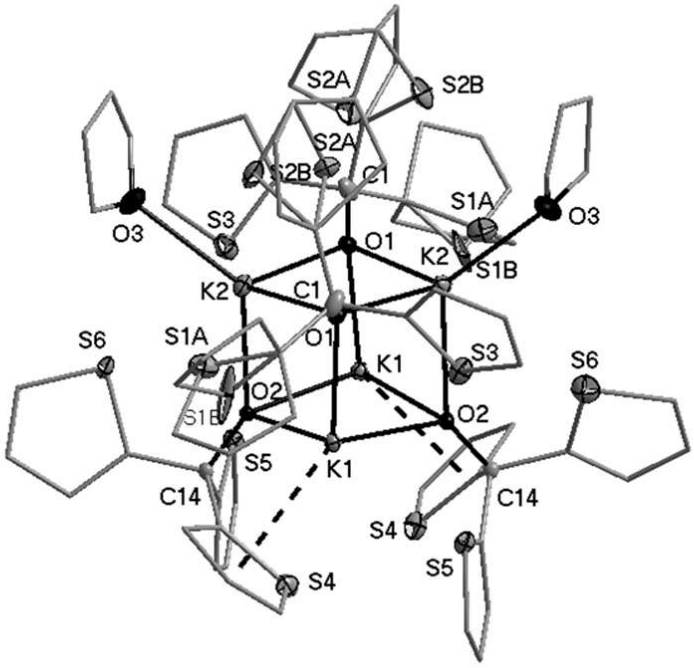

85x63mm (300 x 300 DPI)

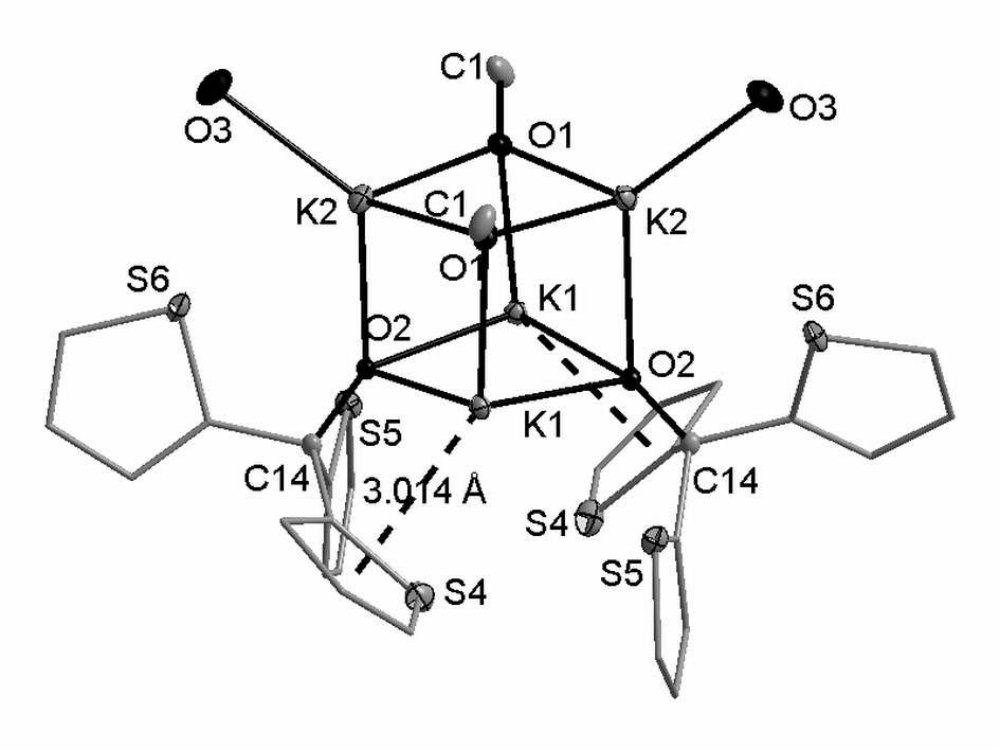

80x60mm (300 x 300 DPI)

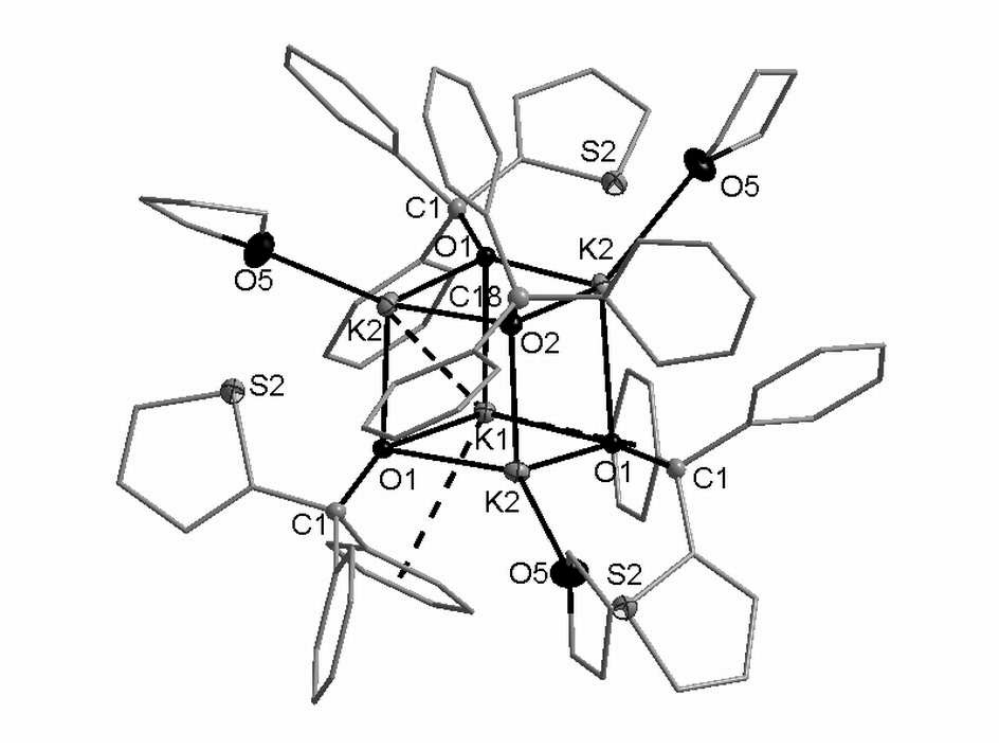

80x60mm (300 x 300 DPI)

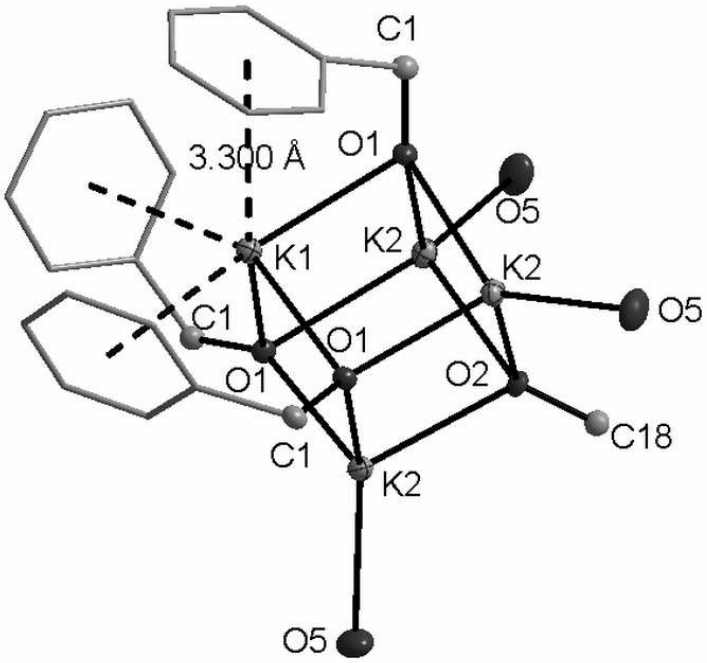

80x60mm (300 x 300 DPI)

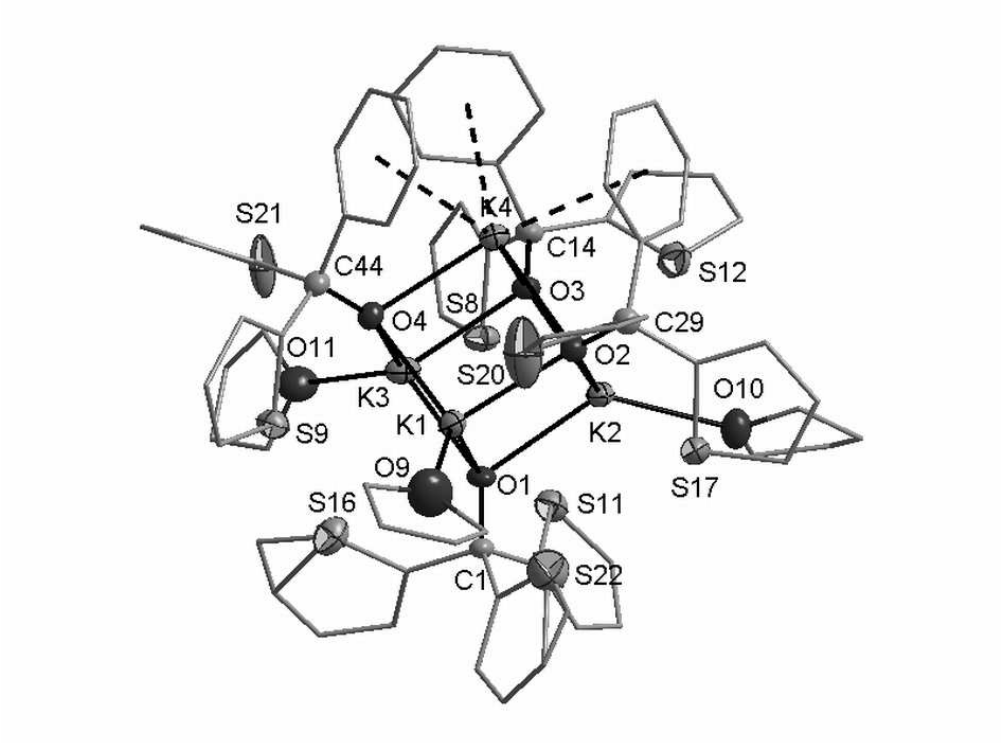

80x60mm (300 x 300 DPI)

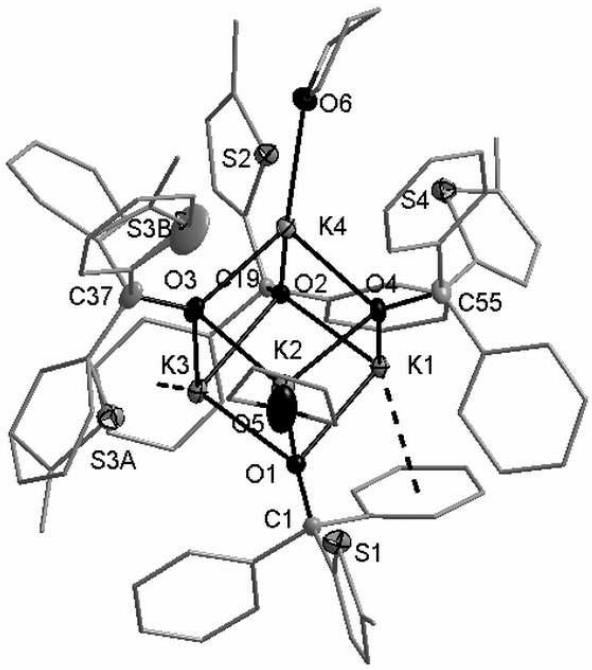

80x60mm (300 x 300 DPI)

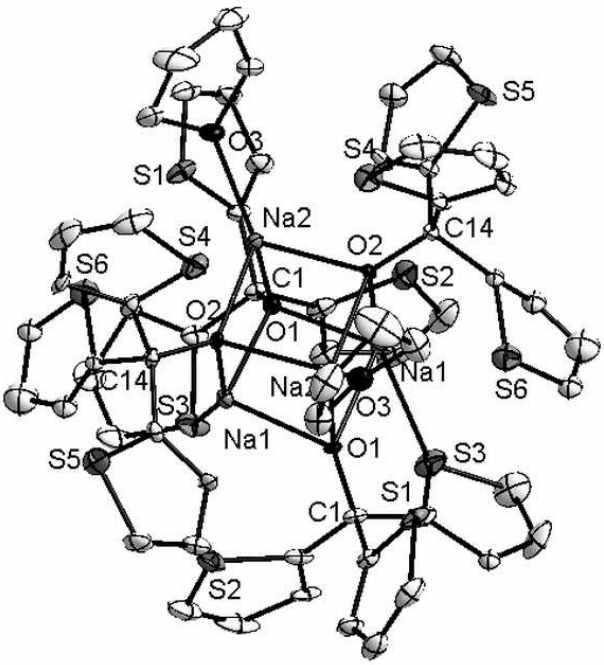

80x60mm (300 x 300 DPI)

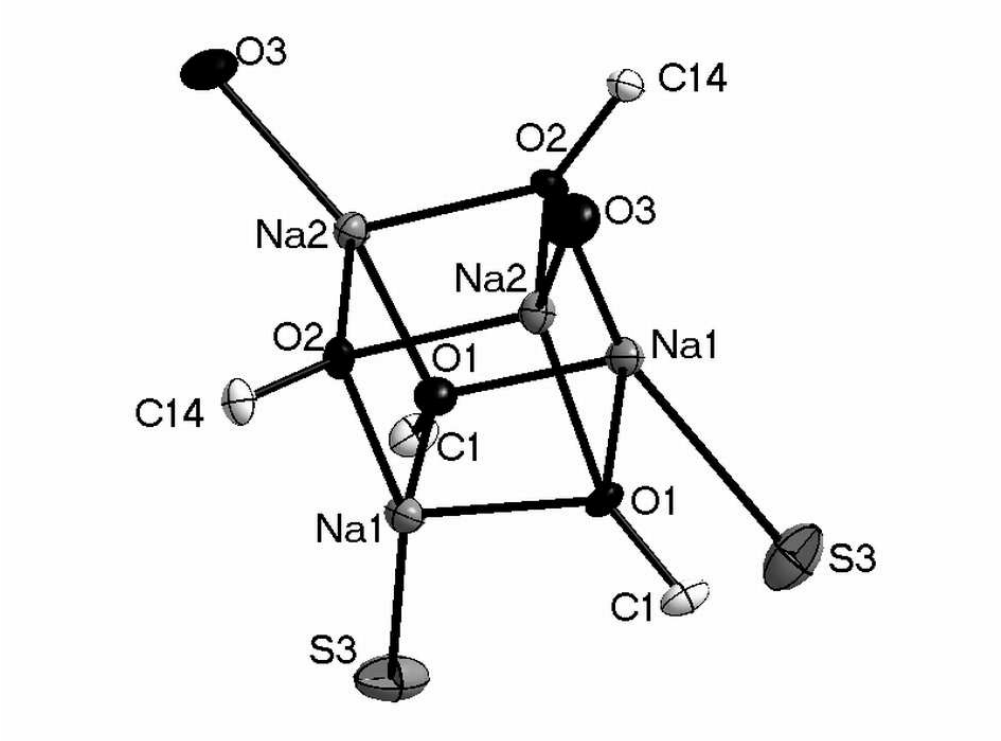

80x60mm (300 x 300 DPI)

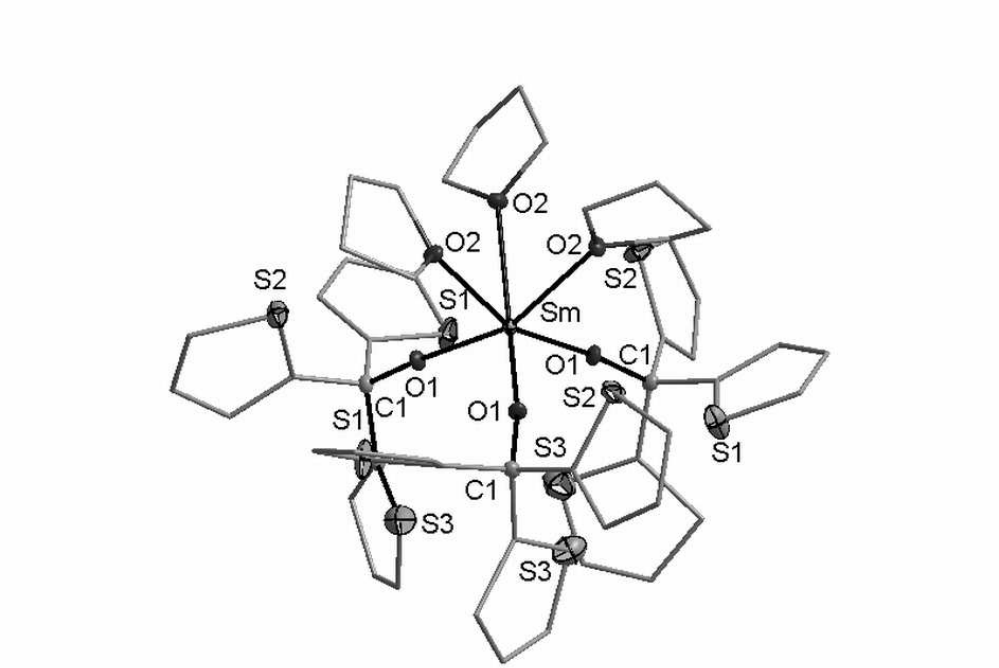

80x60mm (300 x 300 DPI)

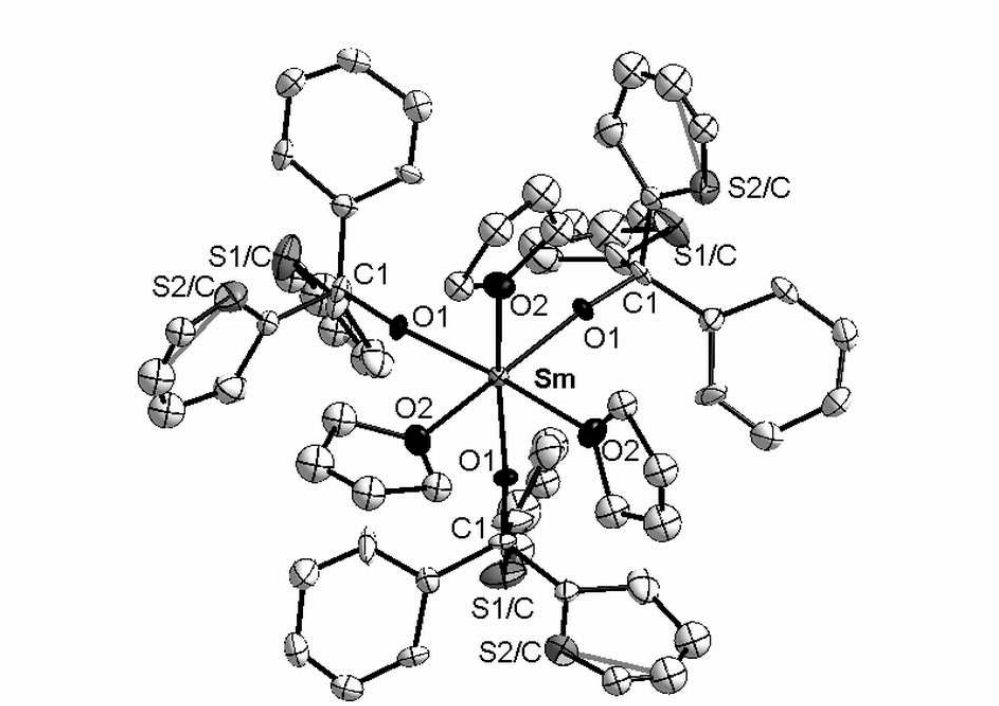

80x60mm (300 x 300 DPI)

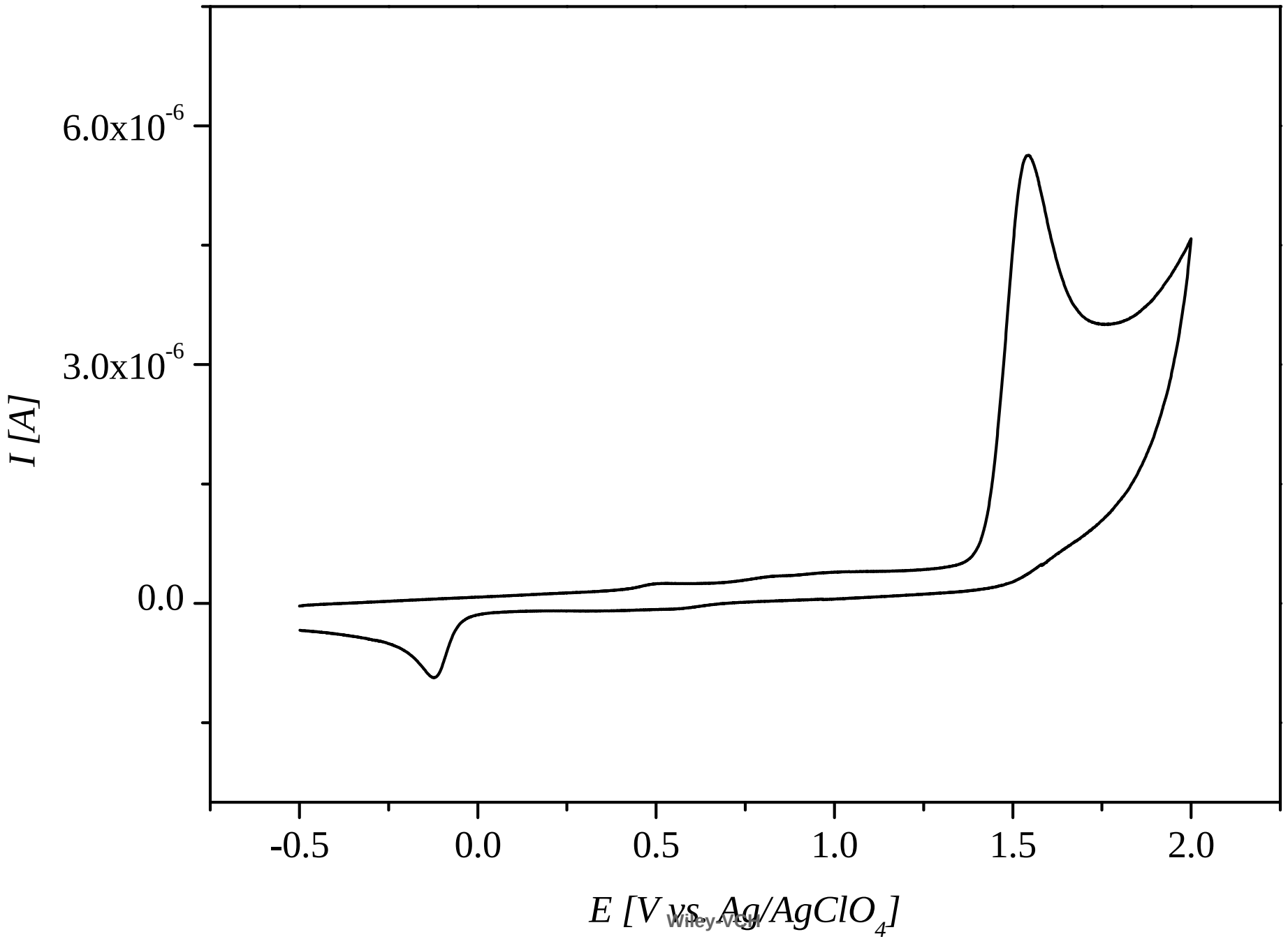

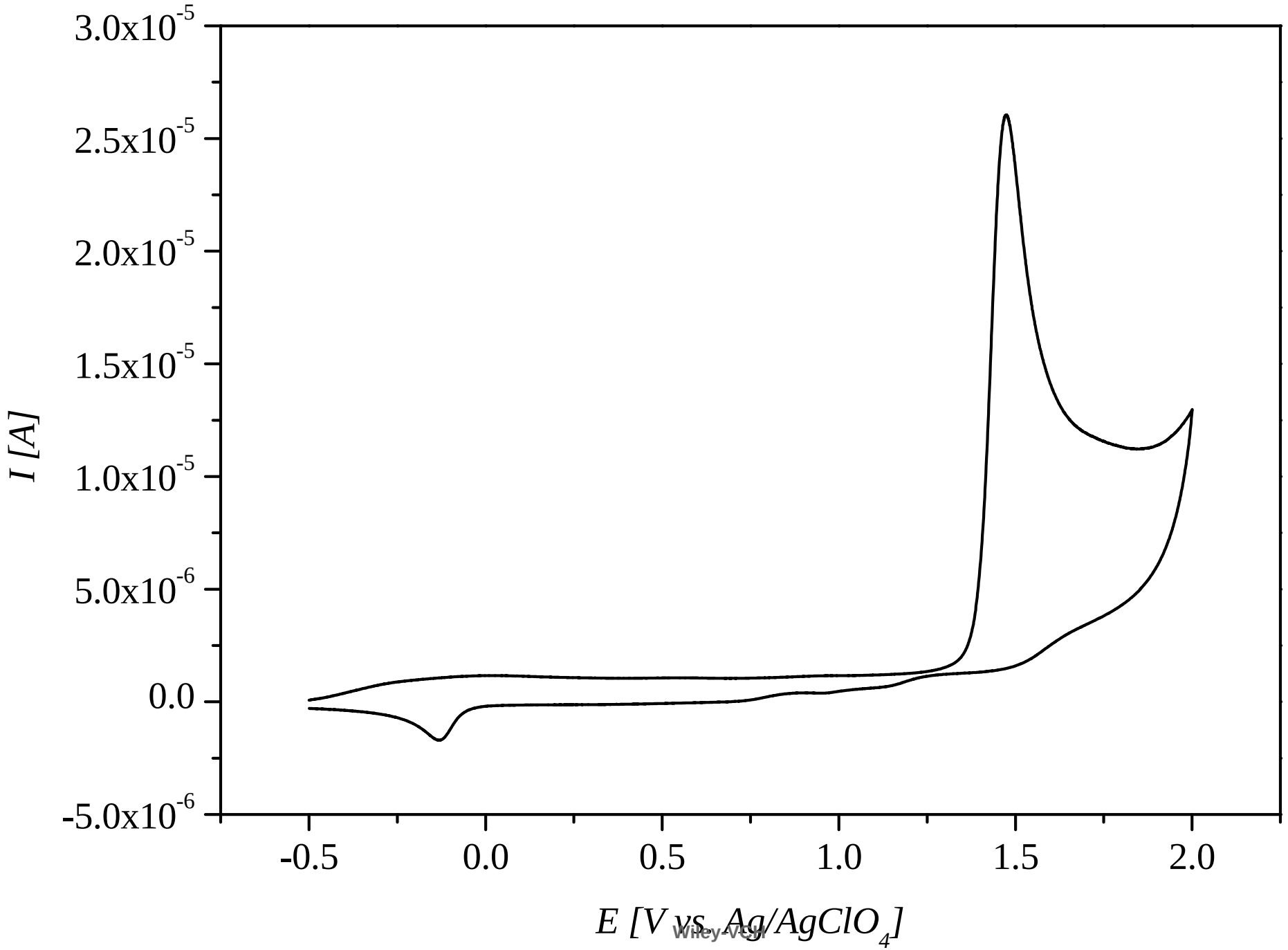
3.0x10-5
2.5x10-5
2.0x10-5
1.5x10-5
1.0x10-5
5.0x10-6
0.0
-5.0x10-6
I [A]
-0.5
0.0
0.5
1.0
1.5
2.0
E [V vs. Ag/AgClO4]

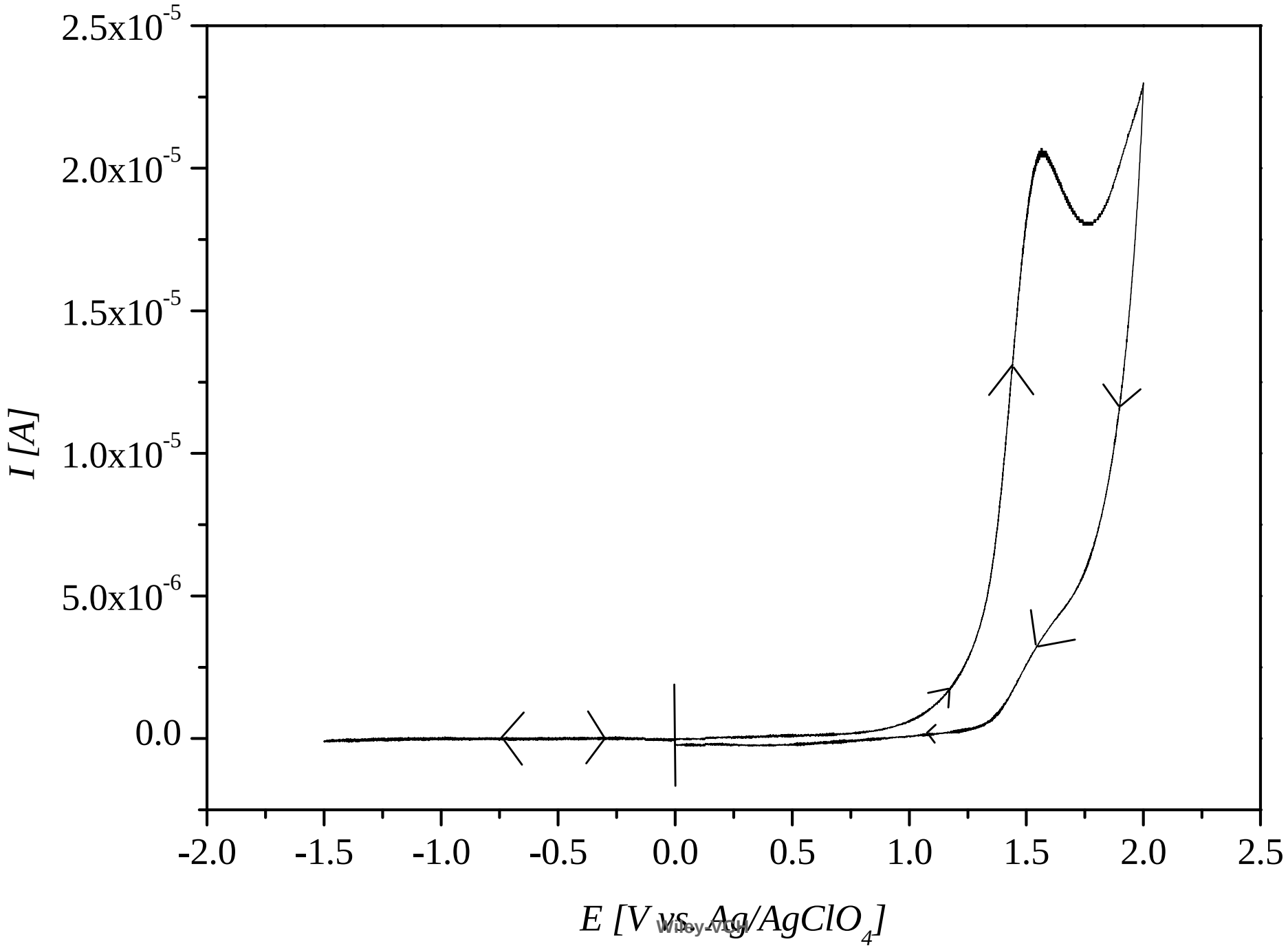
2.5x10-5
2.0x10-5
1.5x10-5
1.0x10-5
5.0x10-6
0.0
I [A]
-2.0
-1.5
-1.0
-0.5
0.0
0.5
1.0
1.5
2.0
2.5
E [V vs. Ag/AgClO4]

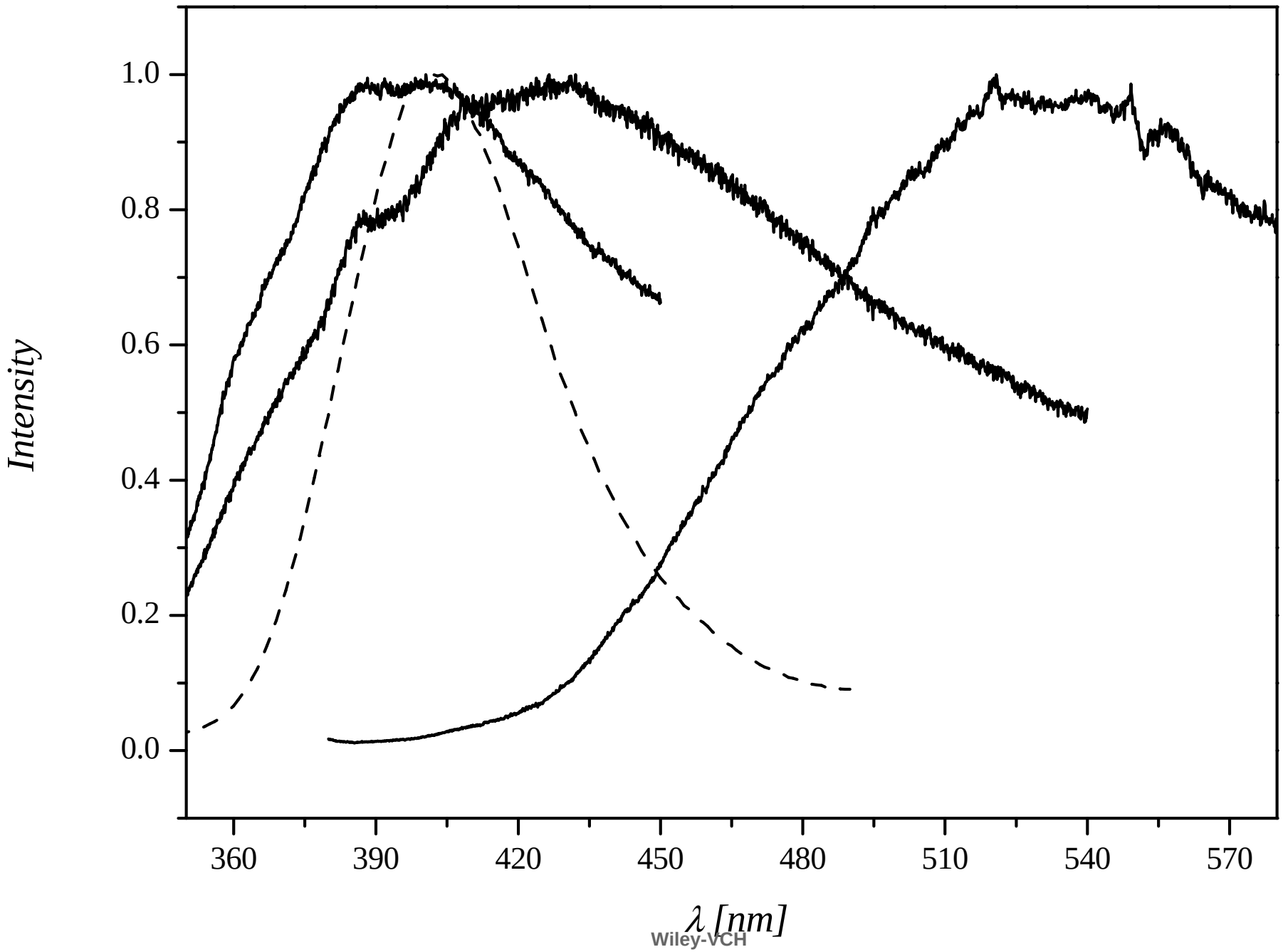
Intensity
1.0
0.8
0.6
0.4
0.2
0.0
360
390
420
450
480
510
540
570
λ [nm]

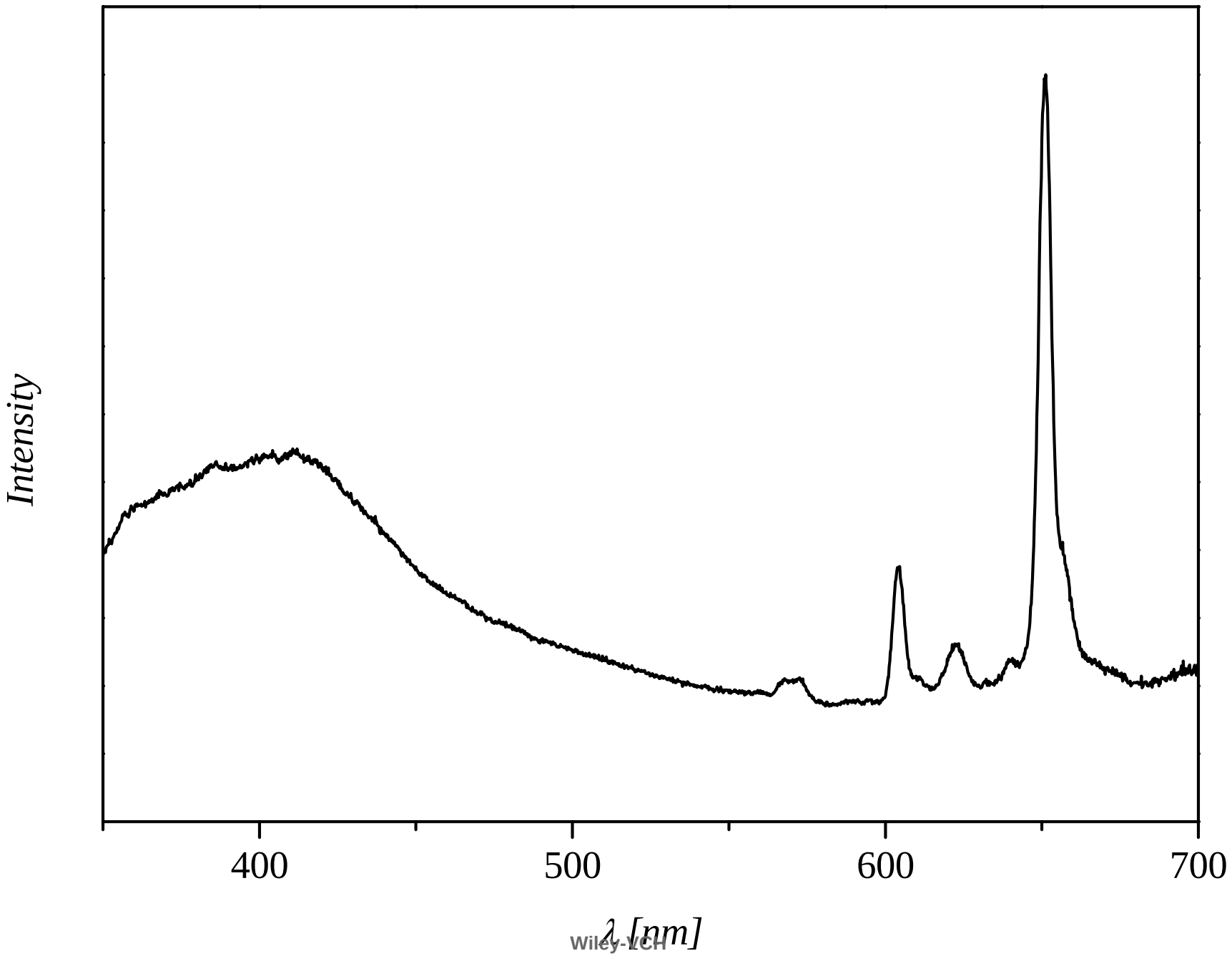

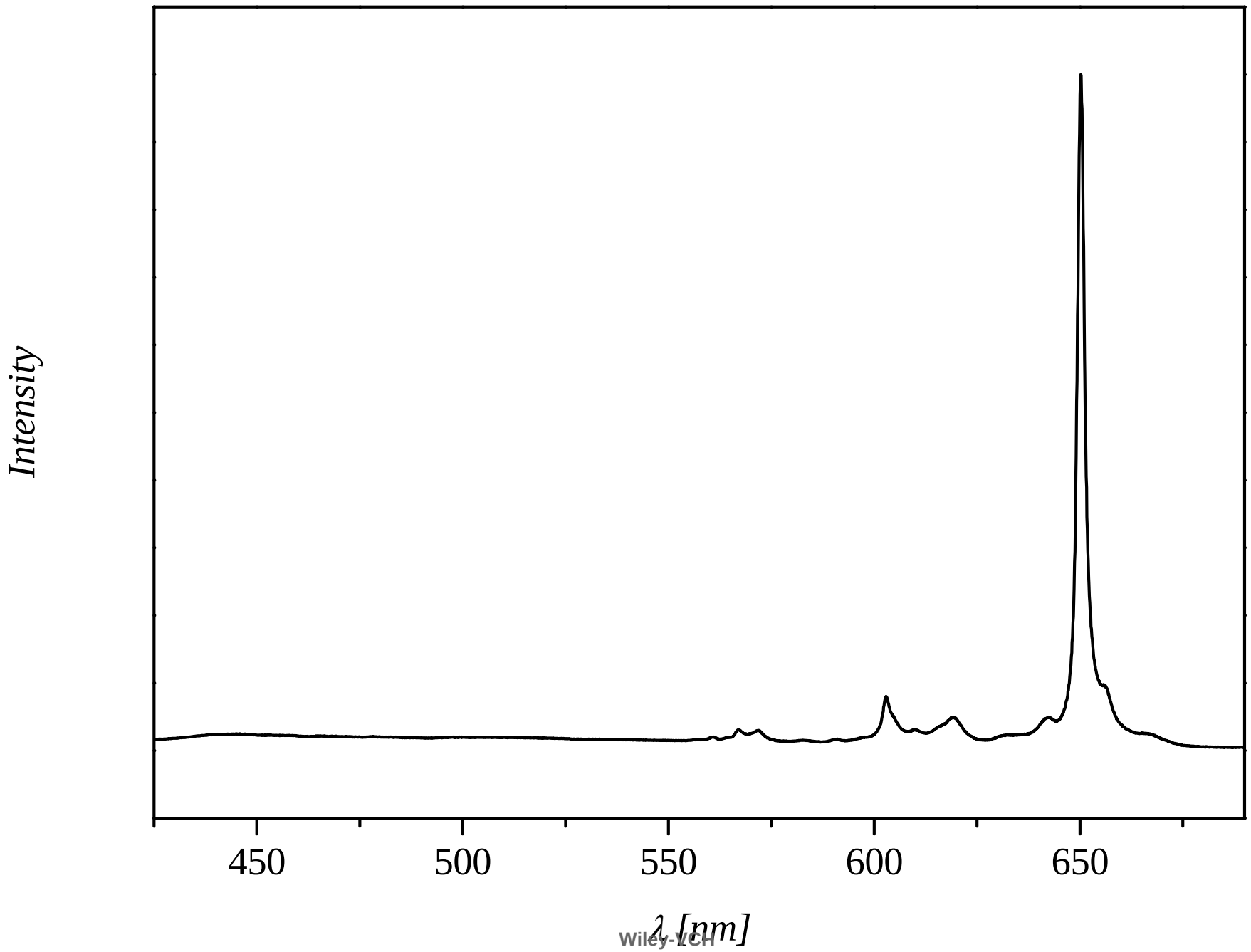

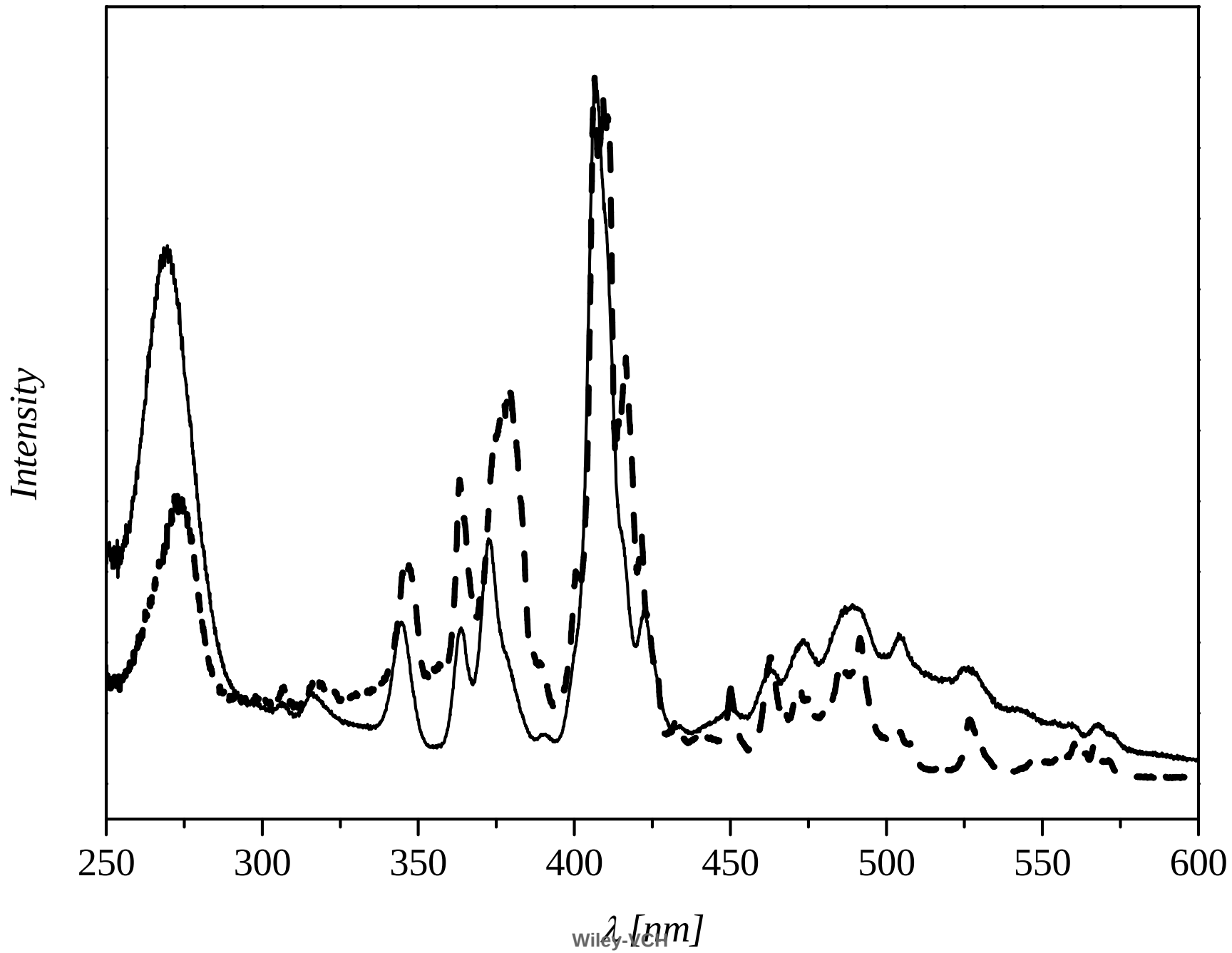

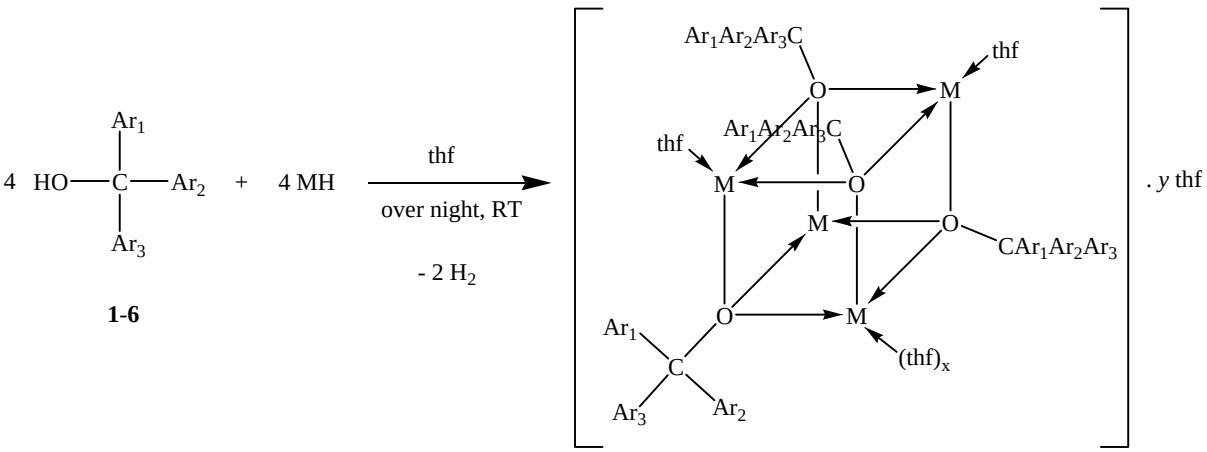

1-6

7-15

Compounds	Ar_1	Ar_2	Ar_3	M	*x*	*y*
7	2–Th	2–Th	2–Th	K	0	1
8	2–Th	2–Th	2–Th	Na	0	0
9	2–Th	2–Th	Ph	K	1	0
10	2–Th	2–Th	Ph	Na	0	0
11	2–Th	Ph	Ph	K	1	½
12	5–Me–Th	Ph	Ph	K	0	0
13	5–Me–Th	Ph	Ph	Na	0	0
14	3–Th	3–Th	Ph	Na	0	0
15	3–Th	Ph	Ph	Na	0	0